Robust control strategy by the Sterile Insect Technique for reducing epidemiological risk in presence of vector migration

Pierre-Alexandre Bliman, Yves Dumont

Robust Control Strategy by the Sterile Insect Technique for Reducing Epidemiological Risk in Presence of Vector Migration

Pierre-Alexandre Bliman[1], Yves Dumont[2,3,4*]

[1]Sorbonne Université, Université Paris-Cité, Inria, CNRS, Laboratoire Jacques-Louis Lions, équipe Mamba, 5 Place Jussieu, 75005 Paris (France),

[2]CIRAD, Umr AMAP, Pôle de Protection des Plantes, F-97410 Saint Pierre, France,

[3]AMAP, Univ Montpellier, CIRAD, CNRS, INRA, IRD, Montpellier, France

[4]University of Pretoria, Department of Mathematics and Applied Mathematics, Pretoria, South Africa

Abstract

The Sterile Insect Technique (SIT) is a promising technique to control mosquitoes, vectors of diseases, like dengue, chikungunya or Zika. However, its application in the field is not easy, and its success hinges upon several constraints, one of them being that the treated area must be sufficiently isolated to limit migration or re-invasion by mosquitoes from the outside. In this manuscript we study the impact of males and (fertile) females migration on SIT. We show that a critical release rate for sterile males exists for every migration level, in the context of continuous or periodic releases. In particular, when (fertile) females migration is sufficiently low, then SIT can be conducted successfully using either open-loop control or closed-loop control (or a combination of both methods) when regular measurements of the wild population are completed. Numerical simulations to illustrate our theoretical results are presented and discussed. Finally, we derive a threshold value for the females migration rate, when viruses are circulating, under which it is possible to lower the epidemiological risk in the treated area, according to the size of the human population.

Keywords: Sterile Insect Technique; migration rates; Periodic impulsive control; Open-loop and closed-loop control; critical release rate

Contents

*Corresponding author: yves.dumont@cirad.fr

1 Introduction

Vector control has become an important challenge throughout the world, as diseases-carrying mosquitoes are spreading and establishing in several parts of the world where a majority of the population is fully susceptible to dengue, chikungunya, zika and other arthropod-borne diseases. It is now a Public Health issue to find appropriate control methods, that is having the property of being sustainable, of impacting only preferentially the targeted vectors, and, of course, of being efficient.

The Sterile Insect Technique (in short, SIT) might verify these three conditions. SIT has been developed since the 1940s. It has been used more or less successfully in the field against various kinds of pests or vectors [11]. Classical or standard SIT consists of mass releases of males sterilized by ionizing radiation. Mating with wild females, these males will transfer their sterile sperms to wild females, resulting in a progressive decay of the targeted population. It is also possible to sterilize mosquito males using either genetics, with the controversial RIDL ("Release of Insects carrying Dominant Lethal gene") technology [20], or *Wolbachia* bacteria [23]. However, whatever the sterilization technique, SIT, while conceptually very simple, is complex to conduct in the field, at an industrial scale. Indeed, it not only requires mass rearing and sterilization facilities, but also necessitates to follow a quite complex protocol, intended to guarantee the quality of the sterile males in terms of competitiveness, lifespan, residual fertility, etc. and to minimize the amount of sterile females inadvertently introduced, through the use of sexing method. Based on these information, releases strategies have to be developed, modelling may become a precious tool to derive control scenarios best fitted to the actual mosquito and epidemiological parameters. Since the places where SIT can be used are quite diverse, it is important to consider models that are, as much as possible, generic, and amenable to theoretical analysis, in order to derive threshold parameters and to find the best combination of parameters values (related, for instance, to the sterile males parameters) to ensure the success of SIT campaigns. Theoretical results are also important because they are helpful to choose adequate numerical algorithm to achieve numerical simulations of SIT systems:

wrong choice in the numerical method can drive to false (numerical) results, misinterpretation, and thus inadequate responses in the field.

In previous works, we highlighted several issues in SIT that were poorly addressed, like *residual fertility* (the fact that sterile males are not 100% sterile) [3], or *accidental release of sterile females* during virus circulation [10], which both have the capacity to drive SIT to failure. Here, we consider the issue of *migration of mosquitoes from the exterior* towards the interior of the domain under treatment, and its negative impact on SIT when this migration is not controlled or mitigated. The present paper extends the results published in [5] to the occurrence of wild mosquitoes migration, as well as the epidemiological analysis provided in [10].

It is now acknowledged that *Ae. albopictus* spreads rapidly, and this fact explains that this species is now well established in Southern Europe and all over the world, while this was not the case a couple of decades ago. However, while global estimates on its annual spread are certainly valuable, it is also quite important to have estimates of its daily behavior, at a local scale. Indeed, the mosquitoes, and in particular the female mosquitoes, are looking for places that will favor their establishment or their growth, seeking either for hosts, breeding sites, matings or resting places. In general, in many publications, it is affirmed that *Ae. albopictus* has a low-dispersal capacity, with a daily Mean Traveled Distance (MTD) between 35 m and 70 m in tropical areas [15], and over 200 m in urban area in temperate regions (see [16, 17] and references in [25]). Other dispersal estimates obtained in [26], using a partial differential approach and Mark-Release-Recapture data, confirm the previous values. However, recent Mark-Release-Recapture studies conducted in Switzerland showed that most of *Ae. albopictus* individuals can travel more than 250 m, and some individuals more than 700 m [25]. Other field experiments, in central Texas, suggest a male-biased dispersal, more precisely that males can disperse farther than females [19]. As indicated in [14], the range of dispersal is influenced by the environment, location, and local strain. This dispersal ability, and thus the migration, is particularly important when the area treated or controlled by SIT is surrounded by one or several areas where intervention is, for some reason, impossible. If the controlled area is not isolated, it is of paramount importance to establish whether the control can be achieved without prior reduction of the migration, or at least to determine what would be, in such an eventuality, the negative impact of this migration on the efficacy of the control.

It is well known that *Aedes albopictus* population fluctuations are due to environmental parameters, like temperature [7], wind, and also rainfall. As an example, in previous modeling works [8, 9], environmental parameters, like temperature or wind were taken into account, as they play a role in the lifecycle of the insect and in the transport of odors attracting mosquitoes, respectively. In particular, the simulations provided in [8] showed that wind direction can impact mosquitos' displacements and thus entail adaptation of the spatialization of the control (SIT) strategies.

On the other hand, integrating variable climate influence is not systematically useful in an entomological models. First, this increases the mathematical complexity of the model, which must be compensated by substantial gain in the description and understanding of the dynamics. Second, most of the temperature or environmental-dependent parameters are deduced from laboratory experiments, during which it is quite difficult to reproduce real environmental conditions. Last, the solution of a model with variable parameters (through, say, the temperature...) can usually be lower and upper bounded by solutions of some constant parameter problems, so that considering extreme constant parameters models may be relevant in practice. This is definitely our option in the present work: our aim is to understand the key phenomena and provide first quantitative outlook, using a simple framework permitting genuine demonstrations of the results and didactic exposition.

Leaving the mosquito population evolve freely leads to population settling at a level characteristic to the carrying capacity of the environment. We present here various control methods, providing more and more realistic description at the price of more and more complex analysis, namely: permanent release of constant amplitude; impulsive periodic releases of constant amplitude; and impulsive periodic releases based on feedback. All of them allow to reduce the male and female populations below some values depending *linearly* upon the migration inflows. We use this analysis to enlighten the existence, for any vector-borne disease, of some migration threshold, above which the epidemic risk cannot be contained.

More precisely, the organization of the paper is as follows. We propose in Section 2 a controlled sex-structured model describing the implementation of Sterile Insect Technique in presence of male and female migration. This model (system (1) below) is an extension of a model previously studied in [5], and constitutes the basis of the paper. Some general properties are provided in the same section. Model (1)

is first applied in Section 3 to study the natural evolution of a mosquito population subject to migration, in absence of treatment by sterile males. Sterile insects are then introduced in the remaining of the paper, to analyze their impact. First, Section 4 considers the effects of constant permanent releases. The reason for considering this setting, admittedly quite unrealistic in practice, is that it allows for a complete study of the mechanisms of SIT, whose analysis is more involved in the more realistic cases studied in the sequel. Section 5 then considers the case of periodic impulsive releases of constant amplitude, and Section 6 the case of periodic impulsive releases of an amplitude computed in accordance with the measure of the wild population at the date of release. Last, Section 7 applies the previous results to the reduction of epidemiological risk by SIT, in presence of migration. Concluding remarks are given in Section 8. Notice that in order to ease readability, all demonstrations have been gathered in Appendix at the end of the paper.

2 Model and properties

The contribution of this section is twofold. First, the model used in this article is introduced in Section 2.1. Second, key properties that relate the evolution of the wild populations to the size of the release rate Λ in general conditions are given in Section 2.2.

2.1 A controlled model for SIT in presence of migration

We first introduce and explain the announced model, extended from [5]. It contains three populations, namely the wild male and female adult mosquitoes M and F, and the sterile males M_S.

$$\dot{M} = r\rho F \frac{M}{M+\gamma M_S} e^{-\beta(M+F)} - \mu_M M + m_M(t), \qquad t \geqslant 0 \tag{1a}$$

$$\dot{F} = (1-r)\rho F \frac{M}{M+\gamma M_S} e^{-\beta(M+F)} - \mu_F F + m_F(t), \qquad t \geqslant 0 \tag{1b}$$

$$\dot{M}_S = \Lambda(t) - \mu_S M_S, \qquad t \geqslant 0 \tag{1c}$$

The positive constants r, ρ and β represent respectively the primary sex ratio, the mean number of eggs deposited per female per day and the effects of competition in the preliminary (aquatic) phases of life. The mean death rates, denoted μ_M, μ_F, μ_S, are also positive. The nonnegative number γ, usually smaller than 1, is the relative reproductive efficiency of the sterile males, compared to the wild males. $\Lambda(t) \geqslant 0$ is the rate of release of the sterile males per time unit.

Remark 1. *Model* (1) *only considers a wild adult stage, taking into account the impact of sterile males in the birth rate terms. We overlooked the non-adult stages, in order to obtain a simple (but not too much) model incorporating migration rates and mathematically tractable. Improvements are of course possible. As an example, the duration of the non-adult stages may be taken into account as a delay τ, as in the following variant of* (1)*:*

$$\begin{cases} \dot{M} = r\rho F_\tau \frac{M_\tau}{M_\tau+\gamma M_{S,\tau}} e^{-\beta(M_\tau+F_\tau)} e^{-\tau\mu_A} - \mu_M M + m_M(t), & t \geqslant 0 \\ \dot{F} = (1-r)\rho F_\tau \frac{M_\tau}{M_\tau+\gamma M_{S,\tau}} e^{-\beta(M_\tau+F_\tau)} e^{-\tau\mu_A} - \mu_F F + m_F(t), & t \geqslant 0 \\ \dot{M}_S = \Lambda(t) - \mu_S M_S, & t \geqslant 0, \end{cases} \tag{2}$$

where $e^{-\tau\mu_A}$ represents the proportion of individuals that survived the non-adult stages, and the index τ in $M_\tau, F_\tau, M_{S,\tau}$ indicates delayed values. The dynamics of this system is more difficult to study, and the benefit in the considered situations, in terms of description accuracy and gains in the definition of the control strategies, must be assessed. This is left for further studies.

Male and female migrations are modeled here through the daily rates $m_M(t)$ and $m_F(t)$. From a technical point of view, we assume that the migration rates are bounded, that is $m_M, m_F \in L^\infty(0,+\infty;\mathbb{R}^+)$, and define the quantities $0 \leqslant m_M^{\text{low}} \leqslant m_M^{\text{high}}, 0 \leqslant m_F^{\text{low}} \leqslant m_F^{\text{high}}$ as

$$m_M^{\text{low}} := \liminf_{t\to+\infty} m_M(t),\ m_F^{\text{low}} := \liminf_{t\to+\infty} m_F(t),\ m_M^{\text{high}} := \limsup_{t\to+\infty} m_M(t),\ m_F^{\text{high}} := \limsup_{t\to+\infty} m_F(t). \tag{3}$$

Last, as in [5], we define the following reduced quantities:

$$\mathcal{N}_F := \frac{(1-r)\rho}{\mu_F}, \qquad \mathcal{N}_M := \frac{r\rho}{\mu_M},$$

and assume that

$$\mathcal{N}_F > 1, \qquad \mu_S \geqslant \mu_M \geqslant \mu_F. \tag{4}$$

The inequality on $\mathcal{N}_F$ is necessary to ensure viability of the species [5]. The two other ones are consistant with observations (and used at the margin to simplify some demonstrations in Section 6).

2.2 General effects of the releases

We first introduce the set of release inputs Λ considered in this paper.

Definition 1. *We call* admissible input *any map Λ defined on $(0,+\infty)$ equal to the sum of a locally integrable nonnegative function and of some Dirac functions with positive weights for which there exists $T>0$ such that*

$$\Lambda_{\text{high}} := \limsup_{t\geqslant 0} \frac{1}{T}\int_t^{t+T} \Lambda(s)\ ds < +\infty.$$

For any admissible input, define $0 \leqslant \Lambda_{\text{low}} \leqslant \Lambda_{\text{high}}$ by

$$\Lambda_{\text{low}} := \liminf_{t\geqslant 0} \frac{1}{T}\int_t^{t+T} \Lambda(s)\ ds \geqslant 0.$$

We now present a result that provides general estimates of the asymptotic values of the population, according to the migration rates. Its proof is given in Section A.1 of the Appendix.

Theorem 1. *For any admissible input Λ and any trajectory of (1), the following properties are true:*

$$\frac{T}{e^{\mu_S T}-1}\Lambda_{\text{low}} \leqslant \liminf_{t\to+\infty} M_S(t) \leqslant \limsup_{t\to+\infty} M_S(t) \leqslant \frac{T}{e^{\mu_S T}-1}\Lambda_{\text{high}} \tag{5a}$$

$$\liminf_{t\to+\infty} M(t) \geqslant \frac{m_M^{\text{low}}}{\mu_M}, \qquad \liminf_{t\to+\infty} F(t) \geqslant \frac{m_F^{\text{low}}}{\mu_F} \tag{5b}$$

$$\limsup_{t\to+\infty} M(t) \leqslant \frac{m_M^{\text{high}}}{\mu_M} + \varphi(\Lambda_{\text{low}}), \qquad \limsup_{t\to+\infty} F(t) \leqslant \frac{m_F^{\text{high}}}{\mu_F} + \varphi(\Lambda_{\text{low}}), \tag{5c}$$

for some decreasing function $\varphi : \mathbb{R}^+ \to \mathbb{R}^+$ vanishing at infinity.

Formula (5a) shows that the asymptotic values of M_S are bounded (from above, resp. below) by asymptotic (upper, resp. lower) bounds on the mean value of Λ on time intervals of a given duration. Formula (5b) indicates that persisting migration of males or females implies persistance of the corresponding population, whatever the releases. This is of course a troublesome constraint in the context of population reduction. Formula (5c) expresses that the male and female populations are bounded from above by quantities that depend upon the lower bound Λ_{low} of the release rate Λ. The function φ introduced in the statement being decreasing, these quantities are at least equal to the constants $\frac{m_M^{\text{high}}}{\mu_M} + \varphi(0), \frac{m_F^{\text{high}}}{\mu_F} + \varphi(0)$ obtained when $\Lambda_{\text{low}} = 0$. But for large enough releases, the population is reduced to the values $\frac{m_M^{\text{high}}}{\mu_M}, \frac{m_F^{\text{high}}}{\mu_F}$, due to the fact that φ vanishes at infinity. These latter values realize the best achievable population reduction, met for very large releases. Notice that, if necessary, an explicit expression of φ may be deduced from equation (A.4), page 28.

We stress the fact that the previous estimates are valid under time-varying migration rates m_M, m_F and release rate Λ. The sequel of the paper is devoted to refining qualitatively and quantitatively these estimates. More precisely, the effects of the releases will be studied in details, first when applied permanently and at a constant rate (Section 4), and then more realistically when applied from time to time with a periodic pace (Sections 5 and 6). In order to gain a precise view of the situation, the migration rates will be taken *constant* in these future developments.

Remark 2. *The map $T \mapsto \frac{T}{e^{\mu_S T}-1}$ is decreasing, with thus a maximal value equal to $\frac{1}{\mu_S}$ when $T \to 0$.*

Remark 3. *One may see from the proof that Theorem 1 does not need to assume that $\mathcal{N}_F > 1$.*

3 Analysis of the entomological model ($\Lambda \equiv 0$)

Putting $\Lambda \equiv 0$ in system (1), the uncontrolled system writes

$$\dot{M} = r\rho F e^{-\beta(M+F)} - \mu_M M + m_M, \qquad t \geqslant 0 \tag{6a}$$

$$\dot{F} = (1-r)\rho F e^{-\beta(M+F)} - \mu_F F + m_F, \qquad t \geqslant 0 \tag{6b}$$

It models the evolution of a population of mosquitoes subjected to migrations of males and females, respectively at non-negative rates m_M, m_F.

We investigate here more particularly the behavior when the rates m_M, m_F are constant and obtain estimates more precise than the general ones given in Section 2.2, which are valid when the latter are time-varying. Section 3.1 studies the equilibrium points of system (6) and their stability. The results are illustrated in Section 3.2 through numerical simulations.

3.1 Equilibrium points and asymptotic behavior of the uncontrolled model

The issue of existence of the equilibrium points of the uncontrolled system (6) is assessed in the following result.

Theorem 2 (Equilibria of the entomological model (6) with migration)**.**
• *If $m_F = 0$, then system* (6) *possesses the equilibrium point (M^{**}, F^{**}), with*

$$F^{**} := 0, \qquad M^{**} := \frac{m_M}{\mu_M}.$$

Moreover, it also possesses an equilibrium point (M^*, F^*) with $F^* > 0$, if and only if

$$\log \mathcal{N}_F > \beta \frac{m_M}{\mu_M}. \tag{7}$$

In this case, the latter is unique and given by

$$F^* := \frac{1}{\left(1 + \frac{\mathcal{N}_M}{\mathcal{N}_F}\right)} \left(\frac{1}{\beta} \log \mathcal{N}_F - \frac{m_M}{\mu_M} \right), \qquad M^* := \frac{\mathcal{N}_M}{\mathcal{N}_F} F^* + \frac{m_M}{\mu_M}. \tag{8}$$

• *If $m_F > 0$, then system* (6) *has a unique equilibrium point (M^*, F^*). The latter is such that $F^* > 0$, and is defined as follows: F^* is the unique positive solution of the equation*

$$\left(\mathcal{N}_F \exp\left(-\beta \left(1 + \frac{\mathcal{N}_M}{\mathcal{N}_F} \right) F^* - \beta \frac{m_M}{\mu_F} + \beta \frac{\mathcal{N}_M}{\mathcal{N}_F} \frac{m_F}{\mu_F} \right) - 1 \right) F^* + \frac{m_F}{\mu_F} = 0, \tag{9a}$$

and M^* is deduced as

$$M^* = \frac{\mathcal{N}_M}{\mathcal{N}_F} \left(F^* - \frac{m_F}{\mu_F} \right) + \frac{m_M}{\mu_M}. \tag{9b}$$

The proof of Theorem 2 is the subject of Section A.2.1 of the Appendix.

We now consider the issue of stability of the equilibrium points previously exhibited. The proof of the next result, Theorem 3, is given in Section A.2.2 of the Appendix.

Theorem 3 (Stability properties of the entomological model (6) with migration)**.**
• *Assume $m_F = 0$. If*

$$\log \mathcal{N}_F < \beta \frac{m_M}{\mu_M}, \tag{10}$$

then the equilibrium point (M^{**}, F^{**}) of (6) *with $F^{**} = 0$ is Globally Asymptotically Stable (GAS).*

On the contrary, if (7) *holds, the previous equilibrium point is unstable, and the positive equilibrium point (M^*, F^*) described in* (8) *is GAS.*
• *Assume $m_F > 0$. The unique equilibrium point (M^*, F^*) of system* (6) *displayed in* (9) *is GAS.*

Thus, in absence of female migration and when $\mathcal{N}_F$ is smaller than the exponential of $\beta\frac{m_M}{\mu_M}$, a unique equilibrium point exists and it is GAS. Being deprived of females, this equilibrium corresponds to the artificial maintenance of a male population without native birth, as a consequence of male migration. When $\mathcal{N}_F$ is larger than this quantity (which is itself larger than 1), then a larger equilibrium appears and is GAS. This is due to the fact that the male migration reduces the viability, through the exponential competition terms present in (1).

In presence of female migration, the situation is simpler, as a unique equilibrium exists and settles under all conditions.

Remark 4. *Inequality* (10) *is quite restrictive, since in general* β *is (very) small, while* $\mathcal{N}_F$ *is large. Thus, in practice, the equilibrium* $(M^{**}, 0)$ *will be (always) unstable.*

3.2 Numerical simulations

We illustrate here the findings in Section 3.1, through phase portraits of (6) for several relevant values of the parameters. For all forthcoming simulations, we consider almost the same parameters values than in [5] (see Table 2, page 53 therein), recalled in Table 1 below. For the parameter ρ, which represents the number of hatched eggs that will enter the larvae compartment, we use estimates obtained in [7]. The parameter γ is related to the Fried competitiveness index [12], equal to $\gamma/(1+\gamma)$. When this index is equal to 0.5, then $\gamma = 1$ and sterile males are as competitive as wild males. This index may take quite different values, according to estimates obtained in [21], we take $\gamma = 1$.

Parameter	**Value**	**Description**	**unit**
ρ	8.15	Oviposition rate of viable hatched eggs per female	day^{-1}
r	0.5	$r : (1-r)$ expresses the primary sex ratio in offspring	-
β	3.93×10^{-4}	Inter-individual competition parameter	Ind^{-1}
μ_M	0.04	Mean mortality rate of wild adult male mosquitoes	day^{-1}
μ_F	0.03	Mean mortality rate of wild adult female mosquitoes	day^{-1}
μ_S	0.04	Mean mortality rate of sterile adult male mosquitoes	day^{-1}
γ	1	Competitiveness of sterile adult male mosquitoes	-
m_M	-	Male migration rate	Ind/day
m_F	-	Female migration rate	Ind/day

Table 1: *Aedes spp* parameter values

Note that the male mortality rate is larger than the female mortality rate, because the male lifespan is shorter than the female lifespan. This is well acknowledged for *Aedes albopictus*, see for instance [7]. With these parameter values, we have $\mathcal{N}_F \approx 135.83$ and $\mathcal{N}_M \approx 101.87$ (in particular, the inequalities in (4) are fulfilled). When $(m_M, m_F) = (0, 0)$, the mosquito population at equilibrium is defined by $E^* = (M^*, F^*)$ with $M^* \approx 5,358$, $F^* \approx 7,144$ mosquitoes per hectare. As observed in the phase portraits, obtained using the software Matlab [18], given in Fig. 1, page 8, migration necessarily impacts the positive equilibrium: having only female migration leads to a large number of females at equilibrium, and the control effort will be more intense. Last, migration of males and females yields a positive equilibrium larger than the equilibrium without migration: this is likely to necessitate an increase of the size of the sterile males releases.

4 Control by permanent release of constant amplitude $\Lambda > 0$

We analyze in this section the effects of release, under the simplistic assumptions that the latter are permanently applied with a *constant* rate $\Lambda > 0$, that is:

$$\dot{M} = r\rho F e^{-\beta(M+F)} - \mu_M M + m_M(t), \qquad t \geqslant 0 \tag{11a}$$

$$\dot{F} = (1-r)\rho F e^{-\beta(M+F)} - \mu_F F + m_F(t), \qquad t \geqslant 0 \tag{11b}$$

$$\dot{M}_S = \Lambda - \mu_S M_S, \qquad t \geqslant 0 \tag{11c}$$

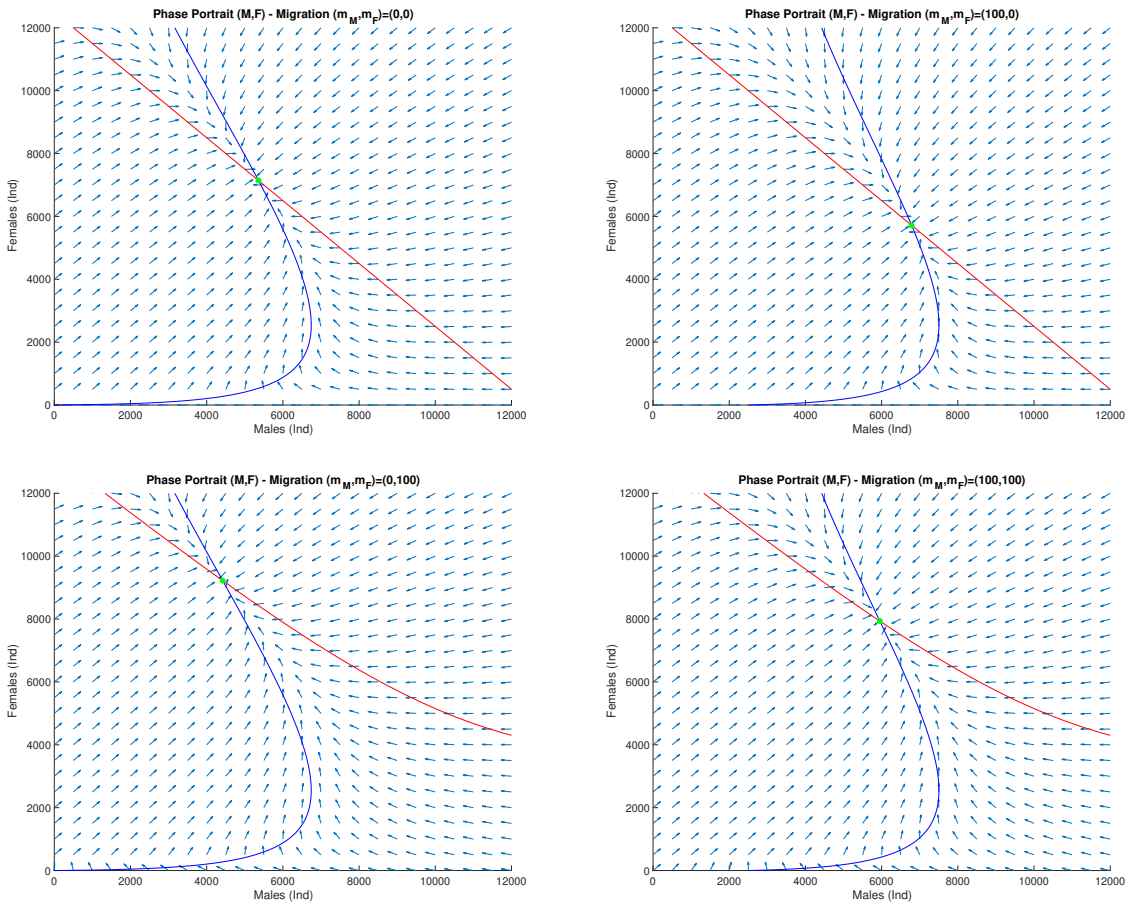

Figure 1: Phase Portrait for model (6), when $\mathcal{N}_F > 1$, in different situations: (a) no migration, (b) with males migration only, (c) with females migration only, (d) with male and female migration.

In such conditions, according to (11c) the number of sterile males converges towards an asymptotic value. One is thus led to consider, instead of (11), the following *stationary* system:

$$\dot{M} = r\rho F \frac{M}{M + \gamma M_S} e^{-\beta(M+F)} - \mu_M M + m_M, \tag{12a}$$

$$\dot{F} = (1-r)\rho F \frac{M}{M + \gamma M_S} e^{-\beta(M+F)} - \mu_F F + m_F, \tag{12b}$$

$$M_S := \frac{\Lambda}{\mu_S}. \tag{12c}$$

As already mentioned at the end of Section 2, we assume that the migration rates $m_M(t), m_F(t)$ are constant in (12), in order to gain tighter estimates than the ones provided in Theorem 1. The existence and stability of the equilibrium points is analyzed in Section 4.1, as a function of the release rate Λ and of the migration rates, and the corresponding findings are illustrated by numerical simulations in Section 4.2.

4.1 Equilibrium points and asymptotic behavior under permanent constant releases

We first recall the following result related to the migration-free case, adapted from [5], see therein the Theorems 1 and 2 for the case $\Lambda = 0$, and the Theorems 3 and 4 for the case $\Lambda > 0$.

Theorem 4 (Equilibrium points in the case $(m_M, m_F) = (0, 0)$)**.** *Assume $\mathcal{N}_F > 1$ and $m_M = 0$, $m_F = 0$.*

There exists $\Lambda^{\text{crit}} > 0$ such that, on top of the zero extinction equilibrium which always exists, (12) *admits two positive distinct equilibria if $0 < \Lambda < \Lambda^{\text{crit}}$, one positive equilibrium if $\Lambda = 0$ or $\Lambda = \Lambda^{\text{crit}}$, and no positive equilibrium if $\Lambda > \Lambda^{\text{crit}}$.*

Moreover, the extinction equilibrium is GAS if $\Lambda > \Lambda^{\text{crit}}$, unstable if $\Lambda = 0$ or $\Lambda = \Lambda^{\text{crit}}$, and LAS whenever $0 < \Lambda < \Lambda^{\text{crit}}$; while when two positive distinct equilibria exist, one of them has larger components than the other and is LAS, while the latter is unstable.

This summarizes the key phenomena in the case where no migration is present. As we will see in the remainder of Section 4.1, the migration only modifies this situation at the margin. We will first characterize the equilibrium points (Section 4.1.1), then determine the equilibrium points in the case where only one migration rate is nonzero (Section 4.1.2), and finally consider the general case $m_M \neq 0$, $m_F \neq 0$ (Section 4.1.3).

4.1.1 Characterization of the equilibrium points

We first study in whole generality the question of the equilibria of (12). Denote

$$a := \gamma M_S = \frac{\gamma\Lambda}{\mu_S}, \quad b := \frac{m_M}{\mu_M}, \quad c := \frac{m_M}{\mu_M} - \frac{m_F}{\mu_F}\frac{\mathcal{N}_M}{\mathcal{N}_F}, \quad d := \beta\left(1 + \frac{\mathcal{N}_F}{\mathcal{N}_M}\right), \quad g := \mathcal{N}_F \exp\left(\beta\frac{\mathcal{N}_F}{\mathcal{N}_M}c\right). \tag{13}$$

Notice that

$$0 \leqslant a, \quad 0 \leqslant b, \quad c \leqslant b, \quad 0 < d, \quad 0 < g. \tag{14}$$

Theorem 4 treated the case where $b = c = 0$, that is $m_F = m_M = 0$, for any value of $\Lambda \geqslant 0$, that is of $a \geqslant 0$. We will now assess the issue of existence of equilibrium points when $(m_M, m_F) \neq (0, 0)$. We first state the following result, which translates the preceding issue into the resolution of a scalar algebraic equation on a given interval.

Lemma 1. *Assume $m_M, m_F \geqslant 0$ with $(m_M, m_F) \neq (0, 0)$. The equilibria of* (12) *are in one-to-one correspondence with the roots of the equation*

$$(x + a)(x - b) = gx(x - c)e^{-dx} \qquad \text{in the interval } [b, +\infty). \tag{15}$$

Lemma 1 is demonstrated in Section A.3.1.

4.1.2 Equilibrium points of (12) for a unique positive migration rate

Recall that we have made the assumption $(m_M, m_F) \neq 0$, that is $(b, c) \neq (0, 0)$. Exploiting the characterization in Lemma 1, we consider now two special cases, before treating the general one in Section 4.1.3.

The case $b = 0 > c$. This case corresponds to $m_M = 0 < m_F$. The solutions of (15) are then exactly $x = 0$, which corresponds to the equilibrium point (M^{**}, F^{**}), with

$$M^{**} := \frac{m_M}{\mu_M} = 0, \qquad F^{**} := \frac{m_F}{\mu_F}; \tag{16}$$

and every solution, if any, of the equation

$$\frac{x + a}{x - c}e^{dx} = g \qquad \text{in the interval } [0, +\infty). \tag{17}$$

The map $x \mapsto \frac{x+a}{x-c}e^{dx}$ admits the derivative

$$\frac{d(x + a)(x - c) - (a + c)}{(x - c)^2}e^{dx} = \left(x^2 + (a - c)x - ac - \frac{1}{d}(a + c)\right)\frac{de^{dx}}{(x - c)^2},$$

whose possible real roots have positive or negative product (as $c < 0 < a$), so that it possesses zero or one local extremum, and (17) may have 0, 1 or 2 positive solutions, according to the parameter values. System (12) may thus have 1, 2 or 3 equilibrium points.

Notice that, for large enough values of a (corresponding to large values of Λ, see (13)), equation (17) has no positive solution, and (M^{**}, F^{**}) defined in (16) is the only equilibrium point of (12).

The case $b = c > 0$. This situation corresponds to $m_M > 0 = m_F$. Here, the solutions of (15) are given by $x = b = c$, yielding the equilibrium point (M^{**}, F^{**}), with

$$M^{**} := \frac{m_M}{\mu_M}, \qquad F^{**} := \frac{m_F}{\mu_F} = 0; \tag{18}$$

plus any solution of the equation

$$\frac{x+a}{x} e^{dx} = g \qquad \text{in the interval } [b, +\infty). \tag{19}$$

The expression in the left-hand side is decreasing and then increasing on $[0, +\infty)$, and as in the previous case, there may 0, 1 or 2 positive solutions to (19), yielding globally 1, 2 or 3 equilibrium points for (12).

Again, only the equilibrium (M^{**}, F^{**}) defined in (18) is present for large values of Λ (represented by large values of a).

The general case, corresponding to $m_M > 0$, $m_F > 0$, is studied in the next Section.

4.1.3 Equilibrium points of (12) in the general case

The case $b \neq c$, $b \neq 0$. This general case corresponds to $m_M > 0$, $m_F > 0$. The solutions of (15) are then the solutions of

$$\frac{(x+a)(x-b)}{x(x-c)} e^{dx} = g \qquad \text{in the interval } [b, +\infty). \tag{20}$$

The analyse of this case is more complicated. It is done through the following auxiliary result, which gathers useful facts. Its proof is given in Section A.3.2.

Lemma 2. *Assume hypothesis* (14) *fulfilled, then*

1. *Equation* (20) *possesses 1, 2 or 3 solutions.*
2. *The largest equilibrium solution of* (20) *is a decreasing function of $a > 0$, and converges towards b when $a \to +\infty$.*
3. *There exists $a^* > 0$ such that for any $a > a^*$, equation* (20) *possesses exactly 1 solution.*

Putting together the results in Lemma 2 (case ($b \neq c$, $b \neq 0$) and the analysis developed in Section 4.1.3 ($b = c$ or $b = 0$), one deduces the following result, which offers a quite clear vision of the effects of constant permanent releases, complementary to Theorem 4.

Theorem 5 (Equilibrium points in the case $(m_M, m_F) \neq (0, 0)$)**.** *Assume $\mathcal{N}_F > 1$ and $(m_M, m_F) \neq (0, 0)$. System* (12) *admits one, two or three equilibrium points.*

Moreover there exists $\Lambda^{\text{crit}} > 0$ such that, for any $\Lambda > \Lambda^{\text{crit}}$, (12) *admits a unique equilibrium point (M^{**}, F^{**}), and*

$$\lim_{\Lambda \to +\infty} (M^{**}, F^{**}) = \left(\frac{m_M}{\mu_M}, \frac{m_F}{\mu_F} \right).$$

Proof of Theorem 5. Theorem 5 is a mere consequence of Lemma 2. The fact that $x \to b$ when $a \to +\infty$ in the latter statement means that $M^{**} \to \frac{m_M}{\mu_M}$ when $\Lambda \to +\infty$. From this and formula (A.15), given in the proof of Lemma 1, one deduces that $F^{**} \to \frac{m_F}{\mu_F}$. □

4.2 Numerical simulations

All forthcoming simulations are done using a standard finite difference method, the ode23tb solver of Matlab [18] which solves system of stiff ODEs using a trapezoidal rule and second order backward differentiation scheme (TR-BDF2) [13, 4].

We estimated the critical rate Λ^{crit} numerically, for each migration sub-cases presented in Fig. 2, page 11. It is quite interesting to observe that to reach the extinction in absence of migration, or to reach the equilibrium (M^{**}, F^{**}) when migration exists, the amounts of sterile males are far different. Without migration, it suffices to choose $\Lambda > \Lambda^{\text{crit}} = 2,138$ Ind/day to drive (more or less rapidly) the wild population to extinction. With migration, the critical value Λ^{crit} is quite different, and indeed much

larger: with male migration only, $\Lambda^{\text{crit}} = 4,988$ Ind/day, with female migration only, $\Lambda^{\text{crit}} = 3,667$ Ind/day, while for the case with male and female migrations, a very large amount is needed to reach (M^{**}, F^{**}), here up to 10^5 Ind/day. In fact, this latter case shows clearly that situations in which migration of both males and females occur may be quite challenging: in such conditions, the wild population is likely to stay quite large, in spite of the releases.

Figure 3, page 12, shows the evolution of Λ^{crit} as a function of m_M and m_F: this value increases rapidly as m_M and m_F increase. This clearly demonstrates that, when too large, the migration can be responsible of SIT failure. Migration control or reduction may thus be needed to achieve successful SIT campaigns, through isolation of the targeted area in order to reduce m_F and m_M as much as possible.

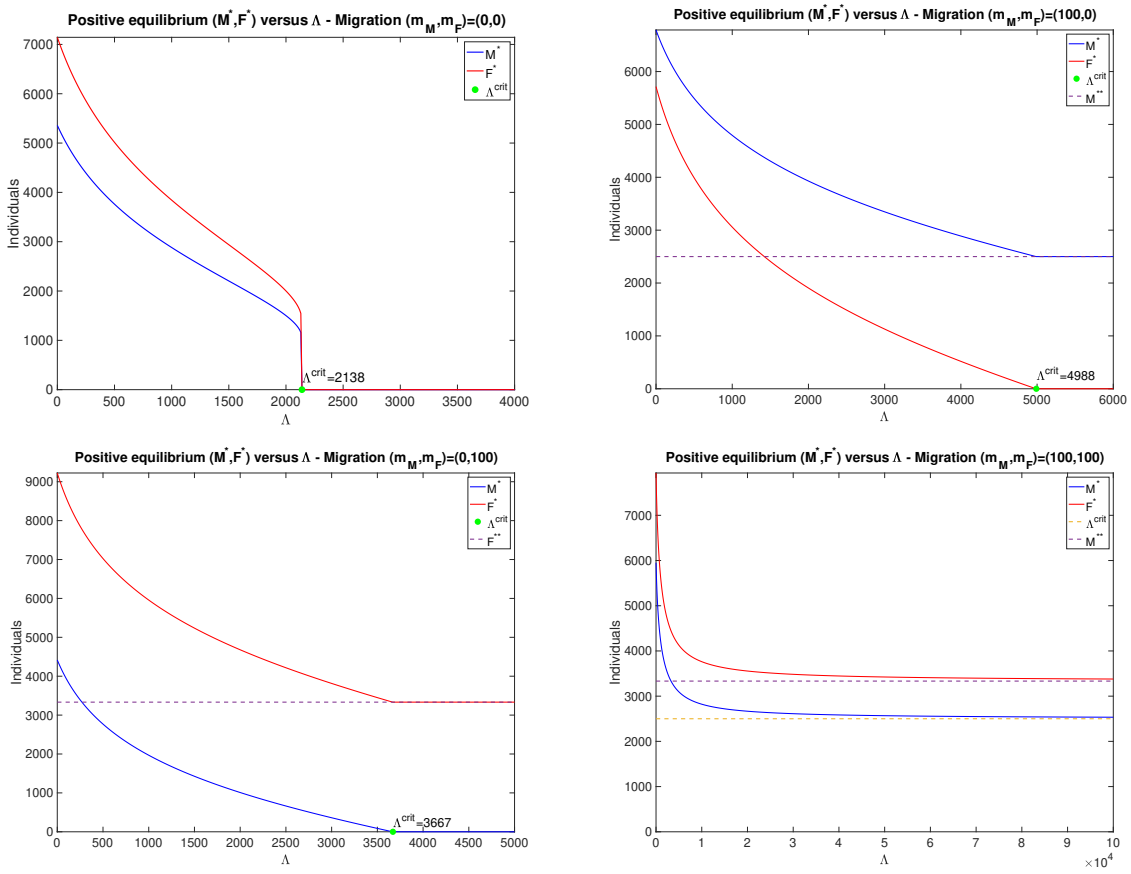

Figure 2: Continuous constant SIT-system (12). Evolution of the positive equilibrium (M^*, F^*) as function of Λ, using (20): (a) no migration, (b) with males migration only, (c) with females migration only, (d) with male and female migration. Λ^{crit}, when reached, is estimated numerically. The dashed lines stand for the migration equilibria $(M^{**}, 0)$, $(0, F^{**})$, or (M^{**}, F^{**}).

5 Control by periodic impulsive releases of constant amplitude

Instead of (12) considered in Section 4, we now discuss the more realistic situation of periodic impulsive releases of period $\tau > 0$ and constant amplitude $\tau\Lambda$, $\Lambda \geqslant 0$. This situation is modelled by the following

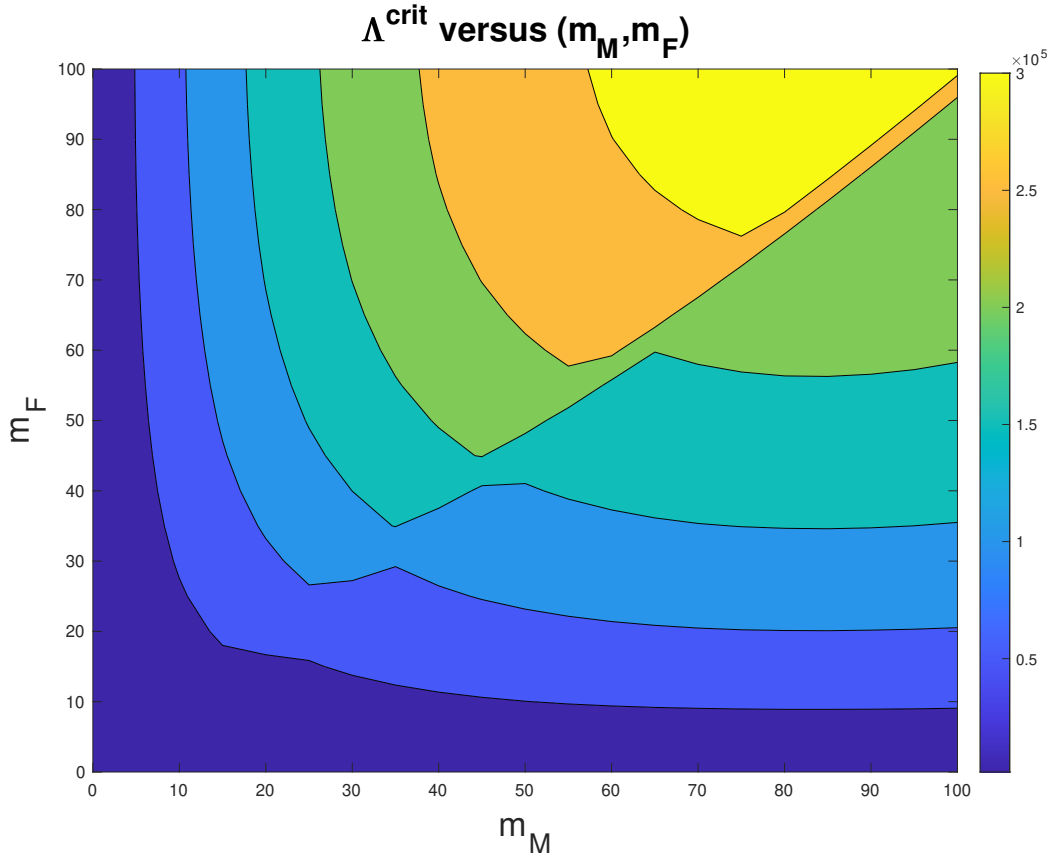

Figure 3: Continuous constant SIT-system (12). Λ^{crit} versus m_M and m_F, for constant continuous releases.

variant of system (1).

$$\dot{M} = r\rho \frac{FM}{M+\gamma M_S} e^{-\beta(M+F)} - \mu_M M + m_M(t), \qquad t \geqslant 0 \tag{21a}$$

$$\dot{F} = (1-r)\rho \frac{FM}{M+\gamma M_S} e^{-\beta(M+F)} - \mu_F F + m_F(t), \qquad t \geqslant 0 \tag{21b}$$

$$\dot{M}_S = -\mu_S M_S \quad \text{for any} \quad t \in \bigcup_{n\in\mathbb{N}} \big(n\tau, (n+1)\tau\big), \tag{21c}$$

$$M_S(n\tau^+) = \tau\Lambda + M_S(n\tau^-), \qquad n = 1, 2, 3, \ldots \tag{21d}$$

The number M_S of sterile males fulfils the piecewise linear differential system (21c)–(21d). The latter admits a unique τ-periodic solution, which may be computed explicitly (see (22c) below) and is globally attracting. One is thus led to study the asymptotic behavior of the following τ-periodic system:

$$\dot{M} = r\rho F \frac{M}{M+\gamma M_S^{\mathrm{per}}(t)} e^{-\beta(M+F)} - \mu_M M + m_M(t), \tag{22a}$$

$$\dot{F} = (1-r)\rho F \frac{M}{M+\gamma M_S^{\mathrm{per}}(t)} e^{-\beta(M+F)} - \mu_F F + m_F(t), \tag{22b}$$

$$M_S^{\mathrm{per}}(t) := \frac{\tau\Lambda e^{-\mu_S\left(t-\lfloor\frac{t}{\tau}\rfloor\tau\right)}}{1-e^{-\mu_S\tau}}. \tag{22c}$$

Asymptotic bounds on the male and female populations are provided in Section 5.1, and illustrated by adequate simulations in Section 5.2.

5.1 Effects of periodic impulsive releases of constant amplitude

The following result, demonstrated in Section A.4, gives ultimate bounds on the trajectories of system (22). Notice in particular that the latter are uniform: they do not depend upon the initial conditions.

Theorem 6 (Sufficient condition for robust control by periodic impulses)**.** *For any given $\tau > 0$, assume that Λ is chosen such that $\Lambda \geqslant \Lambda^{\mathrm{crit}}_{\mathrm{per}}$, where*

$$\tau\Lambda^{\mathrm{crit}}_{\mathrm{per}} := \frac{\cosh(\mu_S\tau) - 1}{\mu_S\tau}\,\frac{1}{e\beta\gamma}\min\left\{2\mathcal{N}_M, 2\mathcal{N}_F, \max\{r, 1-r\}\max\left\{\frac{\mathcal{N}_M}{r}, \frac{\mathcal{N}_F}{1-r}\right\}\right\}. \tag{23}$$

Then there exist two nonnegative vectors $c_{M,\mathrm{per}}(\Lambda), c_{F,\mathrm{per}}(\Lambda) \in \mathbb{R}^2$ such that every solution of system (22) fulfils

$$\limsup_{t\to+\infty} M(t) \leqslant c^{\mathsf{T}}_{M,\mathrm{per}}\begin{pmatrix} m^{\mathrm{high}}_M \\ m^{\mathrm{high}}_F \end{pmatrix}, \qquad \limsup_{t\to+\infty} F(t) \leqslant c^{\mathsf{T}}_{F,\mathrm{per}}\begin{pmatrix} m^{\mathrm{high}}_M \\ m^{\mathrm{high}}_F \end{pmatrix}. \tag{24}$$

Moreover,

$$c_{M,\mathrm{per}}(\Lambda) \geqslant \begin{pmatrix} \frac{1}{\mu_M} \\ 0 \end{pmatrix}, \qquad c_{F,\mathrm{per}}(\Lambda) \geqslant \begin{pmatrix} 0 \\ \frac{1}{\mu_F} \end{pmatrix}, \tag{25a}$$

and one may choose $c_{M,\mathrm{per}}(\Lambda), c_{F,\mathrm{per}}(\Lambda)$ in such a way that

$$\lim_{\Lambda\to+\infty} c_{M,\mathrm{per}}(\Lambda) = \begin{pmatrix} \frac{1}{\mu_M} \\ 0 \end{pmatrix}, \qquad \lim_{\Lambda\to+\infty} c_{F,\mathrm{per}}(\Lambda) = \begin{pmatrix} 0 \\ \frac{1}{\mu_F} \end{pmatrix}. \tag{25b}$$

Precise value of $c_{M,\mathrm{per}}, c_{F,\mathrm{per}}$ may be obtained from the details in proof, see formulas (A.21), (A.25), (A.29) below.

Theorem 6 provides results of the same nature than formula (5c) in Theorem 1, but with tighter estimates. An important feature is that for large enough releases (i.e. $\Lambda \to +\infty$), one obtains

$$\limsup_{t\to+\infty} M(t) \leqslant \frac{m^{\mathrm{high}}_M}{\mu_M}, \qquad \limsup_{t\to+\infty} F(t) \leqslant \frac{m^{\mathrm{high}}_F}{\mu_F},$$

which is the "best possible worst case". Notice also that $\Lambda^{\mathrm{crit}}_{\mathrm{per}}$ does not depend upon the migration rates $m^{\mathrm{high}}_M, m^{\mathrm{high}}_F$.

5.2 Numerical simulations

Using (22c), it is possible to derive a rough value for $\Lambda^{\mathrm{crit}}_{\mathrm{per}}$, like the one obtained for the continuous constant releases in Fig. 2, page 11, by solving (20) with $a = \gamma \min_{[0,\tau)} M^{\mathrm{per}}_S(t) = \gamma\frac{\tau\Lambda e^{-\mu_S\tau}}{1-e^{-\mu_S\tau}}$.

The initial value is taken at $(M(0), F(0)) = (1000, 1000)$ for all simulations. Since the control starts at time $t = 100$ days, the population has sufficient time to reach practically the positive equilibrium, as seen in the Figures.

Fig. 4 shows the value of the positive equilibrium as a function of $\tau\Lambda$, for several values of the migration rates. The decreasingness is apparent, as well as the critical value $\Lambda^{\mathrm{crit}}_{\mathrm{per}}$ The critical values obtained from Fig. 4 are used afterwards for the next simulations, as they allow to select appropriate size for the releases, in order to have $(M^*_{\mathrm{per}}, F^*_{\mathrm{per}})$ close to the migration equilibrium (M^{**}, F^{**}): taking larger values for Λ, that is $\tau\Lambda \gg \tau\Lambda^{\mathrm{crit}}_{\mathrm{per}}$, does not modify the asymptotic values, but only speeds up the convergence.

Fig. 5, page 15, provides simulations of weekly periodic impulsive SIT control for different values of the migration rates. The applied release rates Λ are chosen according to the numerical estimates of $\tau\Lambda^{\mathrm{crit}}_{\mathrm{per}}$ given in Fig. 4, page 14, such that $\tau\Lambda > \tau\Lambda^{\mathrm{crit}}_{\mathrm{per}}$, and their values are indicated in the pictures. Without migration, controlling wild males and wild females is relatively easy in a reasonable amount of time. When only female migration or male migration occurs (Fig. 5(b)-(c)), massive releases are necessary. However, it is interesting to notice that male migration requires larger releases of sterile males, in order to almost eliminate the female population (Fig. 5(b)). Finally, when both male and female migrations occur, i.e. $m_M > 0$ and $m_F > 0$, the combined effect of these migrations is quite detrimental (Fig. 5(d)): even with massive releases, the wild population is maintained. The SIT release effort to reach (M^{**}, F^{**})

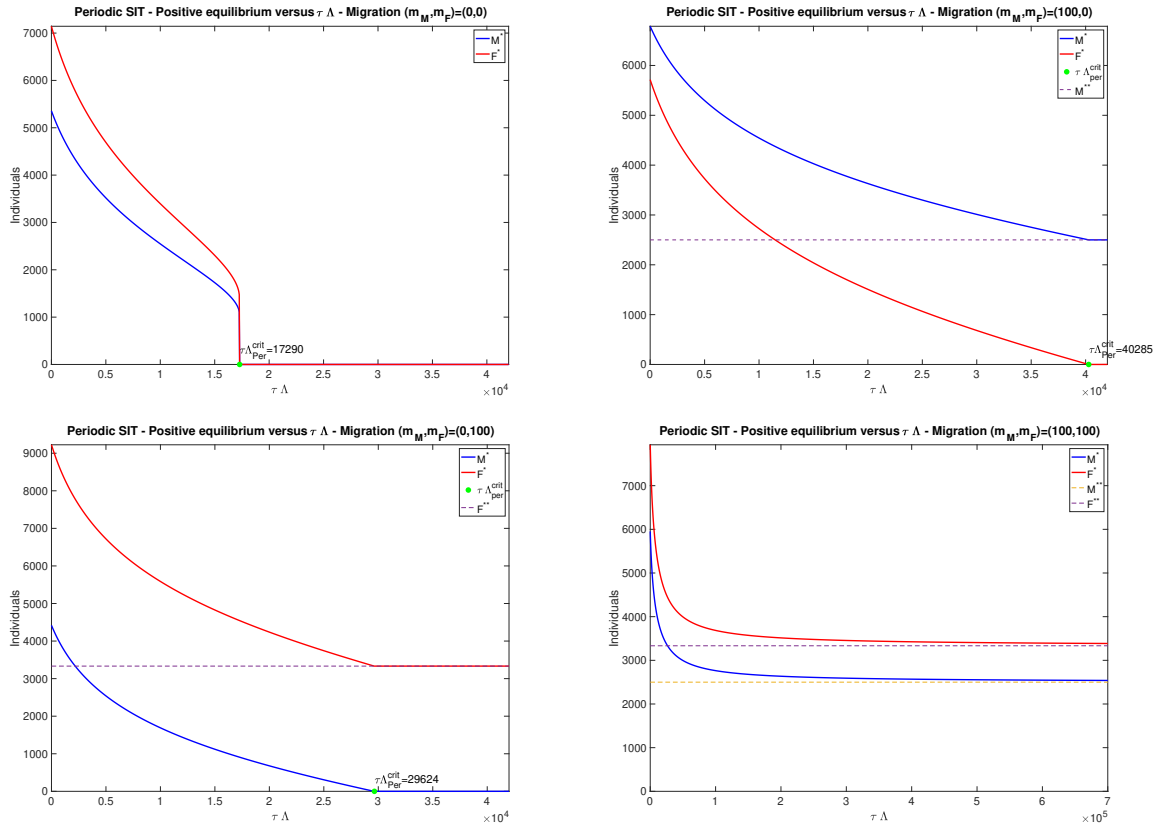

Figure 4: Periodic impulsive SIT-system (22). Open loop control. Evolution of the positive equilibrium (M^*, F^*) as function of $\tau\Lambda_{\text{per}}$: (a) no migration, (b) with males migration only, (c) with females migration only, (d) with male and female migration. The critical parameter $\tau\Lambda_{\text{per}}^{\text{crit}}$ is estimated numerically. The dashed lines stand for the migration equilibria $(M^{**}, 0)$, $(0, F^{**})$, or (M^{**}, F^{**}).

would be so large (see Fig. 5(b), where 10 times more sterile males are released), that it clearly shows the necessity to control or reduce the migrations, in case the latter are important: otherwise, SIT is ineffective.

6 Control by feedback-based periodic impulsive releases

We now consider *periodic impulsive* releases $\Lambda(t)$, modeled by the following variant of system (1):

$$\dot{M} = r\rho\frac{FM}{M+\gamma M_S}e^{-\beta(M+F)} - \mu_M M + m_M(t), \qquad t \geqslant 0 \tag{26a}$$

$$\dot{F} = (1-r)\rho\frac{FM}{M+\gamma M_S}e^{-\beta(M+F)} - \mu_F F + m_F(t), \qquad t \geqslant 0 \tag{26b}$$

$$\dot{M}_S = -\mu_S M_S \ \text{ for any } \ t \in \bigcup_{n\in\mathbb{N}} \big(n\tau, (n+1)\tau\big), \tag{26c}$$

$$M_S(n\tau^+) = \tau\Lambda_n + M_S(n\tau^-), \qquad n = 1, 2, 3, \ldots \tag{26d}$$

Several feedback control laws are proposed in Section 6.1, and their asymptotic properties are established. Related numerical simulations are then shown and analyzed in Section 6.2.

6.1 Feedback-based periodic impulses with sparse measurements

The principle of construction of the feedback control, based on periodic measurement of the ambiant population, is provided in Section 6.1.1. The effect of releasing mosquitoes according to the proposed

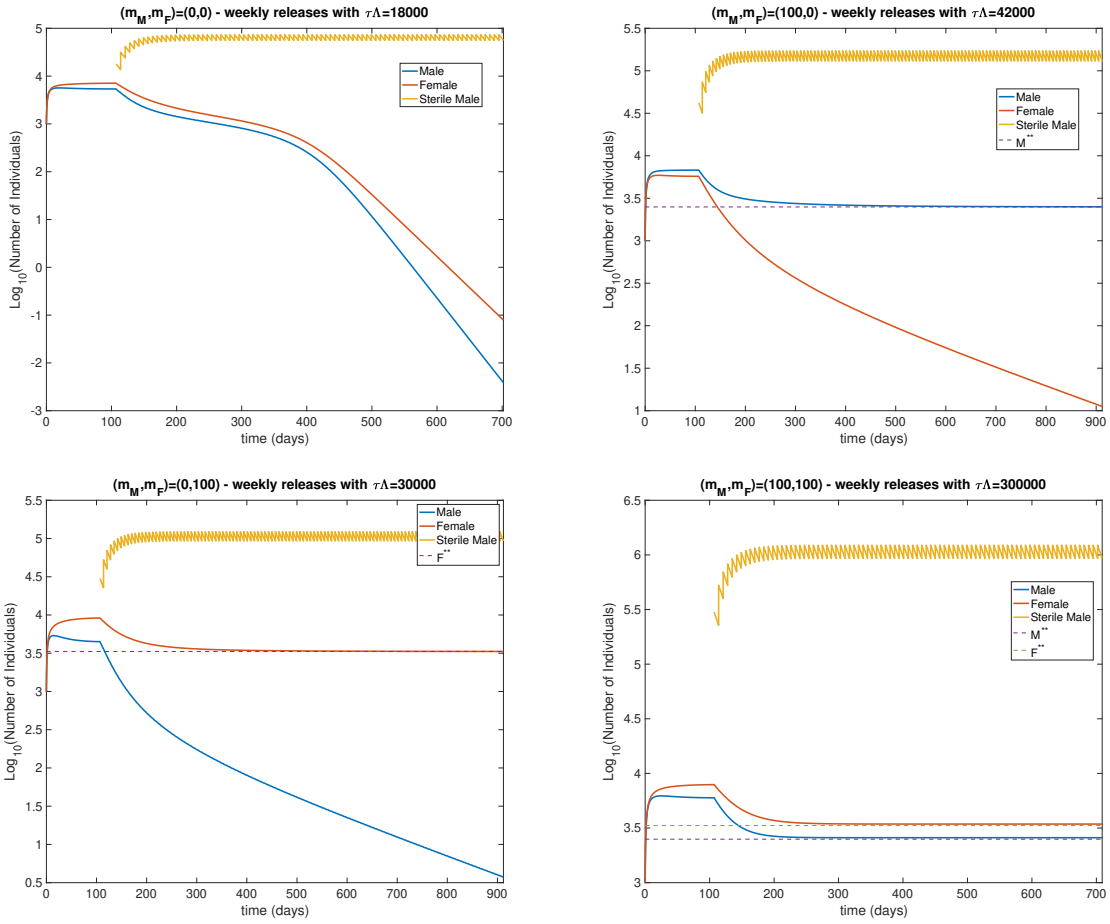

Figure 5: Periodic impulsive SIT-system (22). Open-loop control: (a) no migration, (b) with male migration only, (c) with female migration only, (d) with male and female migration. The dashed lines stand for one of the migration equilibria $(M^{**}, 0)$, $(0, F^{**})$, or (M^{**}, F^{**}).

law is formally stated and demonstrated in Section 6.1.2. Section 6.1.3 is concerned with the amplitude of the control when applying this policy. The result given in Section 6.1.2 is then extended in Section 6.1.4, in order to permit measurement frequency lower than the release frequency, resulting in significant cost reduction. Last, we expose in Section 6.1.5 how saturation of the control may be implemented, in order to reduce the control amplitude peak that appears especially in the beginning of the campaigns, while keeping the desired large-time behavior. This result is obtained on the basis of the findings in Sections 5.1 and 6.1.4.

6.1.1 Principle of the method

The principle of the method that we introduce now is based on two steps. The first one consists in finding out how to obtain desired behavior of the system by adequate direct actuation on M_S. The second one assesses how to produce, through adequate choice of Λ_n, the behavior of M_S prescribed in the first phase.

Step 1 – Setting directly the sterile population level We begin with the following result, demonstrated in Section A.5.1.

Proposition 7. *Let k be a real number such that $0 < k < \frac{1}{N_F}$. Then every solution of (1) such that*

$$\frac{M(t)}{M(t) + \gamma M_S(t)} \leqslant k, \qquad t \geqslant 0 \ , \tag{27}$$

fulfils the following property:

$$\limsup_{t\to+\infty} M(t) \leqslant \frac{1}{\mu_M} m_M^{\text{high}} + \frac{r\rho k}{\mu_M(\mu_F-(1-r)\rho k)} m_F^{\text{high}}, \qquad \limsup_{t\to+\infty} F(t) \leqslant \frac{1}{\mu_F-(1-r)\rho k} m_F^{\text{high}}. \quad (28)$$

Proposition 7 states that, if one succeeds in maintaining permanently below a sufficiently small value the ratio $\frac{M(t)}{M_S(t)}$, then asymptotically the male and female wild population decrease below some levels that are proportional to the external migration intake. These levels, given in the right-hand side of the two inequalities in (28), converge respectively towards $\frac{m_M^{\text{high}}}{\mu_M}$ and $\frac{m_F^{\text{high}}}{\mu_F}$ when the gain k goes to 0. This is coherent with the effects previously observed.

Step 2 – Shaping an impulsive control compliant with Step 1 We now want to ensure that condition (27) is fulfilled, through an adequate choice of the impulse amplitude Λ_n. In virtue of (26c)-(26d), the value of M_S on the interval $\big(n\tau,(n+1)\tau\big]$ is given by

$$M_S(t) = M_S(n\tau^+)e^{-\mu_S(t-n\tau)} = \big(\tau\Lambda_n + M_S(n\tau)\big)e^{-\mu_S(t-n\tau)},$$

and we would like to choose Λ_n in such a way that (27) stays in force. However, instead of computing the (nonlinear) evolution of $M(t)$ on the interval $\big(n\tau,(n+1)\tau\big]$, we will impose, rather than (27), the stronger condition

$$\gamma M_S(t) \geqslant \left(\frac{1}{k}-1\right) M'(t), \qquad t\geqslant 0, \quad (29)$$

where $M'(t)$ refers to the *super-solution* of $M(t)$ introduced in the proof of Proposition 7. The values of M', F' are given analytically by the following statement.

Lemma 3. *The solution of system* (A.30) *on* $(n\tau,(n+1)\tau]$ *with initial values* $\big(M'(n\tau),F'(n\tau)\big) = \big(M(n\tau),F(n\tau)\big)$ *is given by*

$$\begin{pmatrix} M'(t) \\ F'(t)\end{pmatrix} = P(t-n\tau)\begin{pmatrix} M(n\tau) \\ F(n\tau)\end{pmatrix} + Q(t-n\tau)\begin{pmatrix} m_M^{\text{high}} \\ m_F^{\text{high}}\end{pmatrix} \quad (30a)$$

where

$$P(t) := \begin{pmatrix} e^{-\mu_M t} & \dfrac{r\rho k}{\mu_M-\mu_F+(1-r)\rho k}\left(e^{-(\mu_F-(1-r)\rho k)t}-e^{-\mu_M t}\right) \\ 0 & e^{-(\mu_F-(1-r)\rho k)t}\end{pmatrix} \quad (30b)$$

$$Q(t) := \begin{pmatrix} \frac{1-e^{-\mu_M t}}{\mu_M} & \dfrac{r\rho k}{\mu_M-\mu_F+(1-r)\rho k}\left(\frac{1-e^{-(\mu_F-(1-r)\rho k)t}}{\mu_F-(1-r)\rho k}-\frac{1-e^{-\mu_M t}}{\mu_M}\right) \\ 0 & \frac{1-e^{-(\mu_F-(1-r)\rho k)t}}{\mu_F-(1-r)\rho k}\end{pmatrix} \quad (30c)$$

The proof of Lemma 3 is shown in Section A.5.2.

6.1.2 A robust control result

Applying the previous principle and arguing as in [5], it is sufficient, in order to ensure (29), to take

$$\forall s\in[0,\tau], \qquad \gamma\big(\tau\Lambda_n + M_S(n\tau)\big)e^{-\mu_S s} \geqslant \left(\frac{1}{k}-1\right)\begin{pmatrix}1 & 0\end{pmatrix}\left(P(s)\begin{pmatrix} M(n\tau)\\ F(n\tau)\end{pmatrix} + Q(s)\begin{pmatrix} m_M^{\text{high}}\\ m_F^{\text{high}}\end{pmatrix}\right). \quad (31)$$

Assuming as in [5] that the second series of inequalities in (4) holds, it suffices, in order to ensure (31), to verify this inequality at $s=\tau$. One is led, after adequate transformations, to enforce for $n=1,2,\dots,$

$$\tau\Lambda_n \geqslant \left|K\begin{pmatrix} M(n\tau)\\ F(n\tau)\end{pmatrix} + L\begin{pmatrix} m_M^{\text{high}}\\ m_F^{\text{high}}\end{pmatrix} - M_S(n\tau)\right|_+ \quad (32a)$$

$$K := \frac{1}{\gamma}\begin{pmatrix} \frac{1-k}{k}e^{(\mu_S-\mu_M)\tau} \\ \frac{r\rho(1-k)}{\mu_M-\mu_F+(1-r)\rho k}\left(e^{(\mu_S-\mu_F+(1-r)\rho k)\tau}-e^{(\mu_S-\mu_M)\tau}\right)\end{pmatrix}^{\mathsf{T}} \quad (32b)$$

$$L := \frac{1}{\gamma}\begin{pmatrix} \frac{1-k}{k}e^{\mu_S\tau}\frac{1-e^{-\mu_M\tau}}{\mu_M} \\ \frac{r\rho(1-k)}{\mu_M-\mu_F+(1-r)\rho k}e^{\mu_S\tau}\left(\frac{1-e^{-(\mu_F-(1-r)\rho k)\tau}}{\mu_F-(1-r)\rho k}-\frac{1-e^{-\mu_M\tau}}{\mu_M}\right)\end{pmatrix}^{\mathsf{T}} \quad (32c)$$

As a conclusion, one has the following result.

Theorem 8. *For a given $k \in \left(0, \frac{1}{\mathcal{N}_F}\right)$ assume that for any $n \in \mathbb{N}$, Λ_n is chosen according to* (32)*. Then every solution of system* (26) *fulfils property* (28)*.*

Theorem 8 provides a control law that ensures, when enforced, that the wild mosquito population obeys the asymptotic inequalities in (28). It is expressed as a *state-feedback control*, computed from the state $\begin{pmatrix} M(n\tau) & F(n\tau) \end{pmatrix}^{\intercal}$ of the system at the time of the release.

Theorem 8 is indeed an extension of Theorem 10 below and is provided here mostly for didactic purpose. Its proof is subsumed in the proof of the former result.

Remark 5. *Notice that all components of the matrix L tend towards 0 when $\tau \to 0^+$, so that for small values of $\tau > 0$, the right-hand side of* (32a) *only depends upon the value of $M(n\tau), F(n\tau)$. This doesn't mean of course that the lower bound on Λ_n will go to zero when $n \to +\infty$, as $M(n\tau), F(n\tau)$ depend upon the bounds $m_M^{\text{high}}, m_F^{\text{high}}$.*

6.1.3 Asymptotic behavior of the control

Applying the robust control law exposed in Theorem 8 yields ultimate uniform bound on the evolution of the state $\begin{pmatrix} M(t) & F(t) \end{pmatrix}^{\intercal}$. One shows in the following statement that such behavior may be obtained with a control input ultimately uniformly bounded as well. The proof of Theorem 9 is given in Section A.5.3.

Theorem 9. *For a given $k \in \left(0, \frac{1}{\mathcal{N}_F}\right)$, assume that for any $n \in \mathbb{N}$, Λ_n is chosen according to* (32)*,* with equality in (32a) *except possibly on a bounded subset of $\mathbb{R}^+$. Then, for every solution of system* (26)*, one has*

$$\limsup_{n \to +\infty} \Lambda_n \leqslant \Lambda^{\text{feed}}, \qquad \tau \Lambda^{\text{feed}} := \frac{1-k}{\gamma \mu_M} \left(\frac{1}{k} m_M^{\text{high}} + \frac{r\rho}{\mu_F - (1-r)\rho k} m_F^{\text{high}} \right). \tag{33}$$

Notice that, despite some conservatism, the estimate in (33) is linear with respect to the migration rate upper bounds, guaranteeing its nullity when $m_M^{\text{high}} = m_F^{\text{high}} = 0$. On the other hand, it becomes quite imprecise for larger values of k, tending to infinity when the latter gets close to $\frac{1}{\mathcal{N}_F}$.

Define now the values

$$a := \frac{r m_F^{\text{high}}}{(1-r) m_M^{\text{high}}}, \qquad b := \frac{1}{\mathcal{N}_F}, \qquad c := \frac{m_M^{\text{high}}}{\gamma \mu_M},$$

and apply the following result.

Lemma 4. *Let a, b, c be positive real numbers, with $b < 1$. The map*

$$\Phi \ : \ (0, b) \to \mathbb{R}^+, \quad k \mapsto c(1-k) \left(\frac{1}{k} + \frac{a}{b-k} \right)$$

admits a unique minimal value. The latter is reached at

$$k^* := \frac{b}{1 + \sqrt{a(1-b)}}, \tag{34}$$

and is worth

$$\frac{c}{b} \left(\sqrt{a} + \sqrt{1-b} \right)^2. \tag{35}$$

This shows that, when $m_F^{\text{high}} > 0$ and $m_M^{\text{high}} > 0$, there exists a unique smallest value of $\Lambda^{\text{feed}}(k)$ in (33), seen as a function of $k \in (0, \frac{1}{\mathcal{N}_F})$. The latter is attained at

$$k^* := \frac{\sqrt{(1-r) m_M^{\text{high}}}}{\mathcal{N}_F \sqrt{(1-r) m_M^{\text{high}}} + \sqrt{m_F^{\text{high}} \mathcal{N}_F (\mathcal{N}_F - 1)}},$$

and is worth

$$\Lambda^{\text{feed}*} := \frac{\mathcal{N}_F}{\gamma\mu_M}\left(\sqrt{\frac{r}{1-r}m_F^{\text{high}}} + \sqrt{\left(1-\frac{1}{\mathcal{N}_F}\right)m_M^{\text{high}}}\right)^2.$$

Before ending this section, we shortly demonstrate Lemma 4.

Proof of Lemma 4. Rewriting

$$\Phi(k) = c\left(\frac{1}{k} - 1 + \frac{a(1-b)}{b-k} + a\right)$$

and differentiating this expression of Φ, one gets

$$\frac{1}{c}\frac{d\Phi}{dk}(k) = -\frac{1}{k^2} + \frac{a(1-b)}{(b-k)^2}. \tag{36}$$

Therefore, the derivative of Φ is null at $k \in (0,b)$ *iff* $b-k = \sqrt{a(1-b)}k$, that is $k = k^*$ defined in (34). One checks easily that this value pertains to the interval $(0,b)$, and constitutes the unique minimum of Φ in this domain.

Taking advantage of the fact that k^* cancels the right-hand side of formula (36), one has

$$\frac{1}{b-k^*} = \frac{1}{\sqrt{a(1-b)}}\frac{1}{k^*},$$

and thus

$$\begin{aligned}
\Phi(k^*) &= c\left(\frac{1}{k^*} - 1 + \frac{\sqrt{a(1-b)}}{k^*} + a\right) = c\left(\frac{1+\sqrt{a(1-b)}}{k^*} - 1 + a\right) \\
&= c\left(\frac{(1+\sqrt{a(1-b)})^2}{b} - 1 + a\right) = \frac{c}{b}\left(1 + 2\sqrt{a(1-b)} + a(1-b) - b + ab\right) \\
&= = \frac{c}{b}\left(a + 2\sqrt{a(1-b)} + 1 - b\right) = \frac{c}{b}\left(\sqrt{a} + \sqrt{1-b}\right)^2,
\end{aligned}$$

that is (35). □

6.1.4 Extension to the case of sparse measurements

Theorem 8 assumes that measurements and releases are systematically conducted with the same periodicity. In the following statement we generalize this result to the more general situation where the measurements are achieved only once every p releases, for a positive integer p. This extends [5, Theorem 7] in presence of vector migration (and corrects some typos therein).

Theorem 10 (Stabilization by impulsive control with sparse measurements)**.** *Let $p \in \mathbb{N}^*$. For a given $k \in \left(0, \frac{1}{\mathcal{N}_F}\right)$, assume that for any $n \in \mathbb{N}$, $m = 0, 1, \ldots, p-1$, Λ_n is chosen according to*

$$\tau\Lambda_{np+m} \geqslant \left| K_p \begin{pmatrix} M(np\tau) \\ F(np\tau) \end{pmatrix} + L_p \begin{pmatrix} m_M^{\text{high}} \\ m_F^{\text{high}} \end{pmatrix} - M_S(np\tau)e^{-m\mu_S\tau} - \tau\sum_{i=0}^{m-1}\Lambda_{np+i}e^{-\mu_S(m-i)\tau}\right|_+ \tag{37a}$$

$$K_p := \frac{e^{\mu_S\tau}}{\gamma}\begin{pmatrix} \frac{1-k}{k}e^{-(m+1)\mu_M\tau} \\ \frac{r\rho(1-k)}{\mu_M-\mu_F+(1-r)\rho k}\left(e^{-(\mu_F-(1-r)\rho k)(m+1)\tau} - e^{-\mu_M(m+1)\tau}\right) \end{pmatrix}^\intercal \tag{37b}$$

$$L_p := \frac{e^{\mu_S\tau}}{\gamma}\begin{pmatrix} \frac{1-k}{k}\frac{1-e^{-(m+1)\mu_M\tau}}{\mu_M} \\ \frac{r\rho(1-k)}{\mu_M-\mu_F+(1-r)\rho k}\left(\frac{1-e^{-(\mu_F-(1-r)\rho k)(m+1)\tau}}{\mu_F-(1-r)\rho k} - \frac{1-e^{-\mu_M(m+1)\tau}}{\mu_M}\right) \end{pmatrix}^\intercal \tag{37c}$$

instead of (32)*. Then every solution of system* (26) *fulfils property* (28)*.*

As announced previously, one retrieves Theorem 8 by taking $p = 1$ in Theorem 10. The latter is proved in Section A.5.4.

6.1.5 Control by mixed impulsive strategies

A key benefit of the control law exhibited in Section 6.1.4 is its capacity to adapt the amplitude of the release to the size of the wild population present at the time of its achievement. But this method usually yields large amplitudes at the beginning of the treatment. On the other side, releases of constant amplitude like in Section 5.1 guarantee satisfying action with a moderate amplitude. However, by definition, they do not scale to the wild population still present, and may therefore prescribe uselessly large releases. Taking advantage of the assets of both approaches, it is possible to consider, like in [5], a mixed strategy. The latter consists simply in taking the release amplitude equal to the least of the values supplied by the two strategies, namely the value $\Lambda_{\rm per}^{\rm crit}$ given in (23) and the one given by the right-hand side of (37a). The properties of this mixed strategy may be studied like in [5], by use of a common Lyapunov function (of type (A.26)). The details do not present specific interest or originality, and are skipped here for sake of space. However, numerical essays are provided in the sequel, see Section 6.2.2.

6.2 Numerical simulations

We present here numerical essays corresponding to the control with sparse measurements developed in 6.1.4 (Section 6.2.1), and to the mixed control presented in Section 6.1.5 (Section 6.2.2).

6.2.1 Feedback-based impulsive control with sparse measurements

The closed-loop control methods developed in Theorems 8 and 10 ensure the inequalities (28) are fulfilled for any trajectory. Apart from the biological parameters of the model, the latter depend upon the upper bounds $m_M^{\rm high}, m_F^{\rm high}$ on the migration rates, and on appropriate choice of k. Indeed, the smaller k, the larger γM_S, ensuring a substantial decay in the wild population or at least its proximity to the migration equilibrium (M^{**}, F^{**}). On the contrary, if k is close to $\dfrac{1}{\mathcal{N}_F}$, then the decrease in the wild population will be not sufficient, i.e. the latter will not necessarily come close from (M^{**}, F^{**}), except, of course, if $m_F^{\rm high} = 0$. On the other hand, the amount of sterile males to be used to reach this less satisfying result will be smaller than the one dictated by a value of the gain k closer to 0.

It is also important to highlight the important role of female migration in (28). Clearly, if this specific migration can be controlled, i.e. reduced, the control will be tighter, even if male migration arises. This is is directly linked to the fact that the main genuine target of the control, at least for mosquito population, is the female population as only females transmit arboviruses (and, even without this, are source of nuisance through their blood meals).

When $m_F^{\rm high} = m_M^{\rm high} = 0$, (28) confirms that, whatever the choice of $k \in (0, \dfrac{1}{\mathcal{N}_F})$, the system can be driven to 0 (see [5]). Also, as already explained, when $m_F^{\rm high} = 0$, then the wild female population can be driven to 0. However, when $m_F^{\rm high} > 0$ and $m_M^{\rm high} > 0$, then (28) shows that, for large times, the wild population may remain at significant level, generally speaking at least equal to

$$\frac{1}{\mu_M} m_M^{\rm low} + \frac{r\rho k}{\mu_M(\mu_F - (1-r)\rho k)} m_F^{\rm low} \qquad \text{and} \qquad \frac{1}{\mu_F - (1-r)\rho k} m_F^{\rm low}$$

for the male and female populations respectively.

In case of constant migration rates m_M, m_F, the values M_+^{**}, F_+^{**} defined as

$$M_+^{**} = \frac{1}{\mu_M} m_M + \frac{r\rho k}{\mu_M(\mu_F - (1-r)\rho k)} m_F, \qquad F_+^{**} = \frac{1}{\mu_F - (1-r)\rho k} m_F, \tag{38}$$

are such that $M_+^{**} \geqslant M^{**}$ and $F_+^{**} \geqslant F^{**}$. We will illustrate this through the forthcoming simulations.

We first illustrate for a mild migration rates, say $m_F = m_M = 10$ Ind/day, how the choice of the gain k influences the completion of the desired objective. As seen in Figs. 6(a,b), page 20, for small values of k, (M_+^{**}, F_+^{**}) is "close" to (M^{**}, F^{**}); while for large k (that is for k close to, but smaller than, $1/\mathcal{N}_F$), (M_+^{**}, F_+^{**}) remains distant from (M^{**}, F^{**}) (Figs. 6(c,d)). In such situations, while $(M, F) < (M_+^{**}, F_+^{**})$ asymptotically, as predicted by (28), the population levels do not converge to (M^{**}, F^{**}). In addition, Table 6.2.1 shows that reaching (M^{**}, F^{**}), when k is small, has an

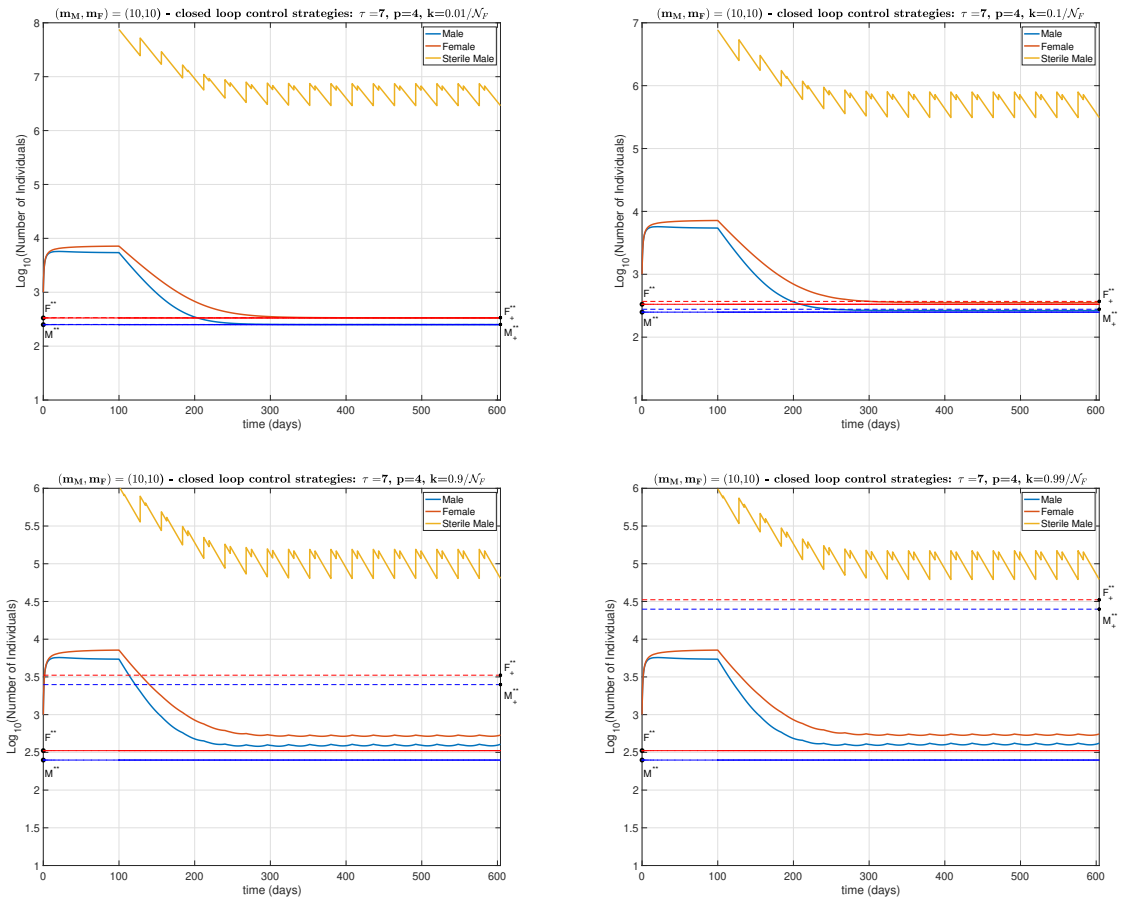

Figure 6: Periodic impulsive SIT-system (26). Closed-loop control for different values of k and $(m_M, m_F) = (10, 10)$. The straight lines stand for the migration equilibrium (M^{**}, F^{**}), while the dotted lines stand for the upper bounds (M_+^{**}, F_+^{**}) given in (38).

important cost in terms of the total amount of released sterile males: around 53 times more sterile males are necessary when k is small ($k = 0.01/\mathcal{N}_F$) than when k is large ($k = 0.99/\mathcal{N}_F$).

When $m_F = 0$ Ind/day and $m_M = 100$ Ind/day, as predicted, M converges to $M_+^{**} \approx M^{**}$, while F converges to 0 whatever k, but more or less rapidly according to k: see Fig. 7, page 21. However SIT control with $k = 0.01/\mathcal{N}_F$ needs 56.74 more sterile males than SIT control with $k = 0.99/\mathcal{N}_F$, even if the duration of the control is shorter.

When $m_F = 100$ Ind/day and $m_M = 0$ Ind/day, F converges to F^{**} whatever k, see Fig. 8, page 21. However, like before, SIT control with $k = 0.01/\mathcal{N}_F$ requires the release of a larger number of sterile males (namely 26.47 times) than the SIT control with $k = 0.99/\mathcal{N}_F$. It is interesting to observe F_+^{**} in Fig. 8(b): F not only verifies (28) but also converges to F^{**}.

6.2.2 Mixed impulsive control

As demonstrated by the previous simulations, migration impacts severely the amount of sterile males to release, in particular when closed-loop control is used, including after the initial decrease of the wild population. In fact, except in the case of (very) small migration rates, the volume of released mosquitoes specified by the closed-loop control method may remain higher than the critical value $\Lambda_{\text{per}}^{\text{crit}}$ prescribed for constant impulsive control. In such situations, the mixed control method may be ineffective, contrary to what occurs in absence of migration, where this method yields appreciable benefits [5]. In Figure 9, page 22, we show the impact of k on the mixed control. Clearly, in order to lower the wild population close to the migration equilibrium, it is necessary to choose k small. Otherwise, when k is large, the system

k	$0.01/\mathcal{N}_F$	$0.1/\mathcal{N}_F$	$0.9/\mathcal{N}_F$	$0.99/\mathcal{N}_F$
Total amount of sterile males	2.0229311256×10^8	2.123998134×10^7	3.7159193×10^6	3.5605414×10^6

Table 2: Total amount of sterile insects over 1000 days for different values of k and $(m_M, m_F) = (10, 10)$.

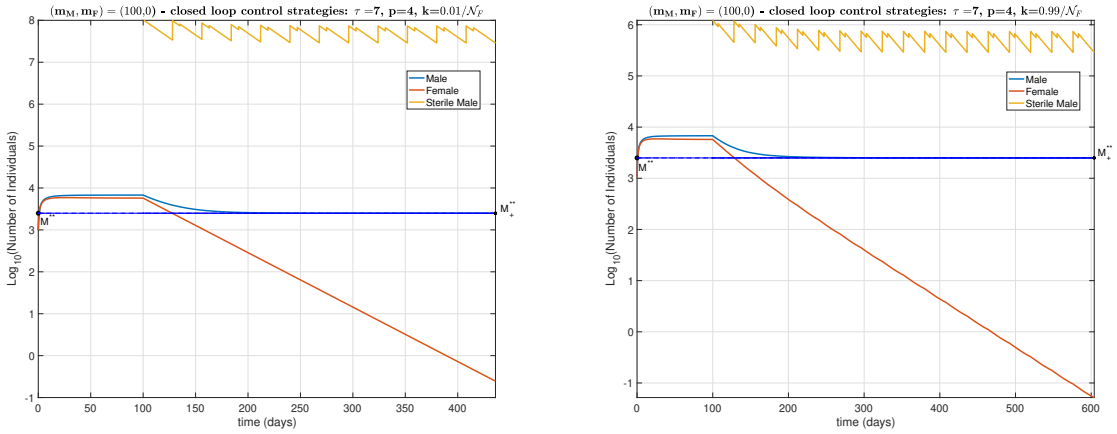

Figure 7: Periodic impulsive SIT-system (26). Closed-loop control for different values of k and $(m_M, m_F) = (100, 0)$. The straight lines stand for the migration equilibrium $(M^{**}, 0)$, while the dotted lines stands for the upper bounds $(M_+^{**}, 0)$ defined in (38).

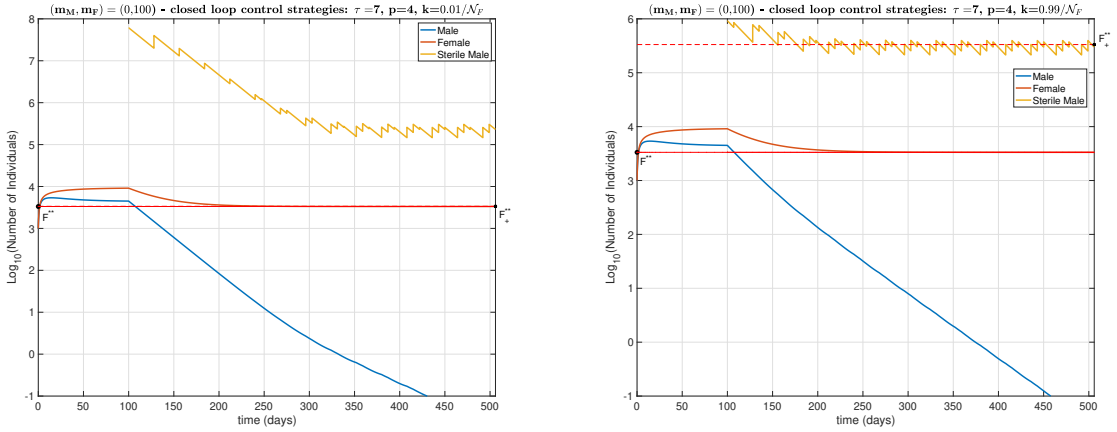

Figure 8: Periodic impulsive SIT-system (26). Closed-loop control for different values of k and $(m_M, m_F) = (0, 100)$. The straight lines stand for the migration equilibrium $(0, F^{**})$, while the dotted lines stands for the upper bounds $(0, F_+^{**})$ given in (38).

switches from open-loop control to closed-loop control, and asymptotically (M, F) verifies (28), but does not converge to (M^{**}, F^{**}): the size of the wild population is still large, even for small migration rate. For larger values of the migration, open-loop control is systematically chosen, with $\tau\Lambda = 21,000$ for these simulations. This shows that the closed-loop method is really useful once the wild population has become small enough, through initial massive releases with the open-loop method, and, of course, when the migration rates are not too large.

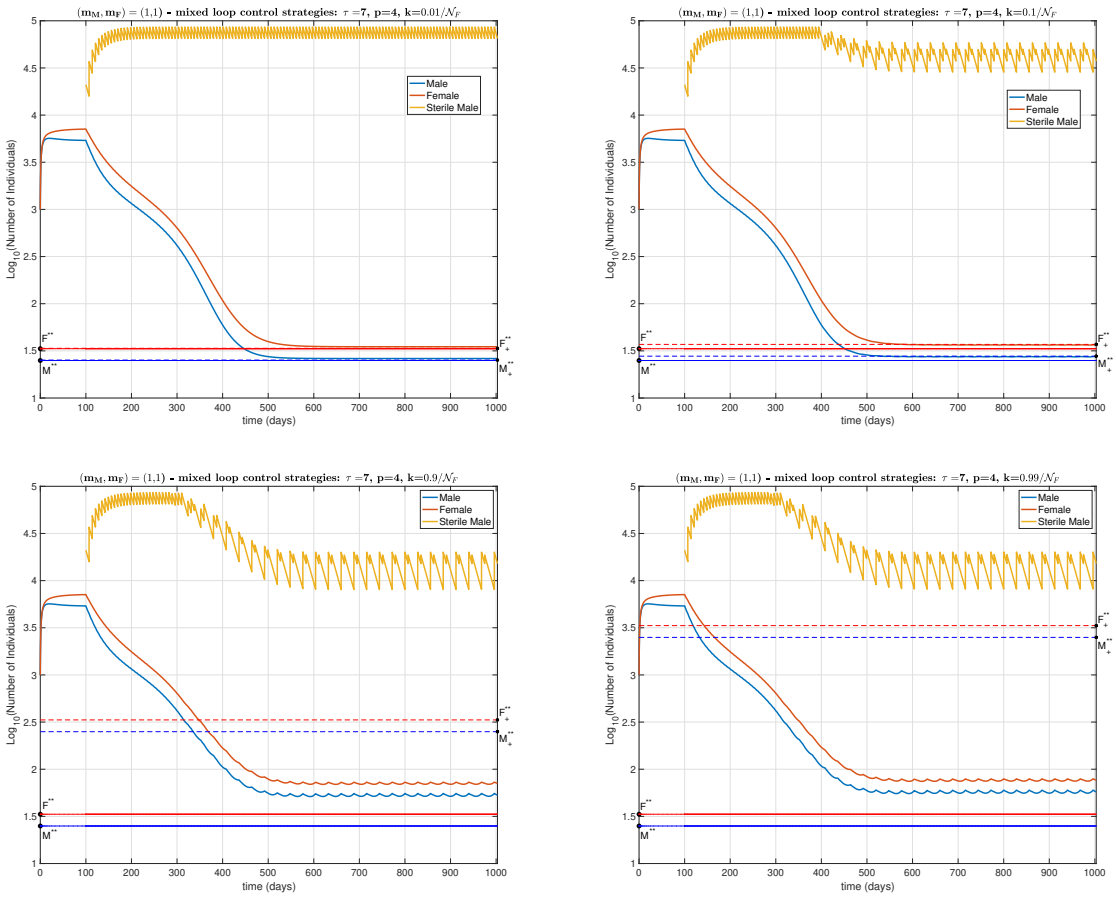

Figure 9: Period SIT mixed-loop control for different values of k and $(m_M, m_F) = (1, 1)$. The straight lines stand for the migration equilibrium (M^{**}, F^{**}), while the dotted lines stands for the upper bounds (M_+^{**}, F_+^{**}) given in (38).

7 Reduction of the epidemiological risk in presence of migration

Sterile Insect Technique is not only useful to prevent or control the establishment of mosquitos, it is also essential to reduce the epidemiological risk when an (arthropod) virus, like dengue or chikungunya, is circulating, carried by vector population of mosquitoes (*Aedes aegypti* and *Aedes albopictus* in the case of these diseases). In order to tackle this important application of SIT, we now consider the implementation of the methods previously exposed to mitigate epidemiological risk. Following [10], we consider more precisely the following SIR-SEI model of dengue transmission, like e.g. in La Réunion island, in the case where only one strain of Dengue is circulating.

The evolution of the human population is given by the following SIR model:

$$\dot{S}_h = \mu_h N_h - \beta_v F_I \frac{S_h}{N_h} - \mu_h S_h, \tag{39a}$$

$$\dot{I}_h = \beta_v F_I \frac{S_h}{N_h} - (\eta_h + \mu_h) I_h, \tag{39b}$$

$$\dot{R}_h = \eta_h I_h - \mu_h R_h, \tag{39c}$$

where S_h, I_h, R_h represent respectively the susceptible, infected and recovered (and permanently immune) human population. The positive parameter μ_h represents the mortality and natality rate. No disease-induced mortality is assumed, so that the total human population is assumed to have reached stationary level $N_h > 0$ (and $1/\mu_h$ represents the average lifespan of human). The parameter β_v is the daily transmissible biting rate [1]. Last, $1/\eta_h > 0$ is the average viremic period.

Extending the model of evolution of the mosquito population described in the previous sections, we use here the following SEI model for the wild mosquitoes (which, as before, is a controlled model subject to male and female migrations), adapted from (1):

$$\dot{M} = r\rho \frac{M}{M + \gamma M_S(t)} e^{-\beta(M+F_S+F_E+F_I)}(F_S + F_E + F_I) - \mu_M M + m_M(t) \tag{40a}$$

$$\dot{F}_S = (1-r)\rho \frac{M}{M + \gamma M_S(t)} e^{-\beta(M+F_S+F_E+F_I)}(F_S + F_E + F_I) - \beta_v F_S \frac{I_h}{N_h} - \mu_F F_S + m_F(t) \tag{40b}$$

$$\dot{F}_E = \beta_v F_S \frac{I_h}{N_h} - (\nu_m + \mu_F) F_E \tag{40c}$$

$$\dot{F}_I = \nu_m F_E - \mu_I F_I. \tag{40d}$$

Last, the evolution of the sterile males is described by the following formula:

$$\dot{M}_S = \Lambda - \mu_S M_S \tag{41}$$

As before M and M_S denote respectively the wild and sterile males. For the female mosquitoes, one distinguished between the susceptible, exposed and infected females, denoted respectively F_S, F_E, F_I. Their mean mortality rates are denoted respectively μ_F, μ_E, μ_I (while μ_M, μ_S represent respectively the mean mortality rates of the wild and sterile males). The constant $1/\nu_m > 0$ represents the average extrinsic incubation period, and the other parameters of the model have the same meaning than in model (1). Our aim is to study the evolution, from an epidemiological point of view, of system (39)-(40)-(41).

We consider for example the framework of permanent releases developed in Section 4 (taking constant values for the male and female migration rates m_M, m_F), and study the behavior around the disease-free equilibrium with mosquitoes defined by

$$(S_h, I_h, R_h) = (N_h, 0, 0), \qquad (M, F_S, F_E, F_I) = (M^*, F^*, 0, 0), \tag{42}$$

where (M^*, F^*) characterizes the equilibrium point of system (12).

Using the next generation matrix approach, straightforward computations lead to the basic reproduction number $\mathcal{R}_0$ of the disease-free equilibrium of system (39)-(40)-(41) (see for instance [24] for further details of the derivation), given as

$$\mathcal{R}_0^2 = \frac{\nu_m {\beta_v}^2}{(\nu_m + \mu_F)\,\mu_I\,(\eta_h + \mu_h)} \frac{F^*}{N_h}.$$

It has been shown in the previous sections that in any case, at an equilibrium point one should have

$$F^* \geqslant \frac{m_F}{\mu_F}.$$

For the more realistic case where the migration rates depend upon time, it has been established (Theorem 1) that, for any trajectory,

$$\liminf_{t \to +\infty} F(t) \geqslant \frac{m_F^{\text{low}}}{\mu_F}.$$

As a corollary, one deduces the key fact that *one cannot control the epidemics if*

$$\frac{\nu_m {\beta_v}^2}{(\nu_m + \mu_F)\,\mu_I\,(\eta_h + \mu_h)} > \frac{\mu_F N_h}{m_F^{\text{low}}}. \tag{43}$$

Formula (43) is quite an appreciable result, as it gives, as a function of characteristics of the life cycle of the mosquitoes and of the transmission of the vector-borne disease, the maximal female migration rate for which the epidemic may be maintained below the epidemic threshold with the help of Sterile Insect Technique, thanks to the size of human population, N_h.

Using the numerical values borrowed from [10] and recalled in Table 3, page 24, one gets numerically:

$$m_F^{\text{low}} > 4.57 \times 10^{-2} \times N_h$$

Symbol	β_v	μ_F	μ_I	ν_m	μ_h	η_h	N_h
Value	0.375	0.03	0.03	1/8	$1/(365 \times 78)$	1/7	$2,000$
Unit	day^{-1}	day^{-1}	day^{-1}	day^{-1}	day^{-1}	day^{-1}	Ind

Table 3: *DENV* epidemiological parameter values (extracted from [1, Table 2])

i.e. for $N_h = 2,000$ inhabitants,

$$m_F^{\text{low}} > 92 \text{ individuals day}^{-1},$$

to be compared with $F^* = 7,144$ individuals per ha.

It is important to emphasize that the rates of migration between distinct locations can be very different in practice, according to environmental parameters and the life cycle of the adult mosquitoes [8, 9]. Indeed, after mating with males, females are seeking for blood meals before going to rest. Afterwards, they start seeking for breeding sites to deposit eggs. Thus depending at which stage they are within the gonotrophic cycle, female mosquitoes have a different behavior and thus a different spreading/migration behavior. Clearly, in places where the number of human hosts is large (villages, cities), they dramatically attract female mosquitoes looking for blood meals, and the (female) migration rate can be large. For male mosquitoes, the objective is to mate and transfert their sperms, so that they look for places to find females, typically near hosts or breeding sites. As indicated in the introduction, so far, the mean spreading distance for *Ae. albopictus* is considered to be between 100 and 200 meters. In fact, they can spread faster, and the issue of migration has to be considered. Unfortunately, field experiments to study this phenomenon, including its fluctuations along the year and its relation with the biological state of the insects, are quite few. Our theoretical results and the related simulations show that this issue is indeed an important issue to be studied for the success of SIT campaigns.

Remark 6. *As explained previously, we considered constant parameters values to derive our preliminary results. Taking into account environmental parameters, like temperature and rainfall, will most certainly show changes between years and within years. This could be done numerically, at least, and is left for further studies. We also have developed a SIT-entomological temperature-dependent model (in preparation) where rainfall is taken into account in the (time) evolution of the aquatic carrying capacity, through the breeding sites. We show that in places like Réunion, rainfall is crucial in the dynamics because it can vary drastically within a year (and even between years), and an SIT treatment can be successful or not, last a long time or not, according to the period of the year where it has started.*

8 Conclusion

According to our knowledge, migration is rarely studied in SIT modeling while, from the experimental point of view, it can be responsible of SIT failures. In this work, we showed that wild population with "small" migration can be controlled by SIT (in addition with other control methods). An important point is that having too large migration rates can be problematic from the epidemiological point of view: even with small amount of female mosquitoes in the targeted area, female migration has the capacity to maintain a high epidemiological risk, i.e. to keep the basic reproduction number $\mathcal{R}_0$ above 1.

Thus, to the extent that migration, and in particular female migration, is important, it is necessary to consider "buffer zones" around the targeted area, in order to minimize the entry of external insects. In this buffer zones, sterile insects may be released in combination with the use of other control tools, including traps (ovitraps and adult traps), mechanical control to reduce te breeding sites, etc. From the experimental point of view, either the targeted area is naturally isolated, like for motu or islands; or, when the targeted area is large, it is necessary to consider corridors where SIT are released to contain the arrival of wild insects and to protect the targeted area, like in [2].

Last, our work also emphasizes the importance of being able to estimate the migration rates in the field, in order to have the capacity to provide an effective control strategy and thereby increase the chance of success of SIT. Such migration rate estimates could be done by, for instance, Mark-Release-Recapture [6, 15], in order to estimate flux between the targeted area and its neighborhood. This kind of experiment is long and difficult, and not necessarily successful, but it seems necessary in order to

minimize the risk of SIT failure and to set-up appropriate buffer zones to reduce the migration rates in the domain under treatment.

A precious outcome of the project TIS 2B "SIT feasibility project against *Aedes albopictus* in Réunion Island" (2020-2022), jointly funded by the French Ministry of Health and the European Regional Development Fund (ERDF), is that estimation the migration rates is an important but difficult issue to conduct in the field. Migration in SIT being a complex issue, our model constitutes a first step towards its understanding and importance. However, we firmly believe that more complex models should be developed, for instance to take into account buffer zones, and the fact that sterile males, released in the targeted domain, can also leave the domain and, thus, have an impact in the buffer zones or in the neighboring domains, reducing thereby the migration of fertile females.

Acknowledgments

Preliminary results of this work have been presented during the workshop on SIT modeling, organized in Réunion island from the 27th of November till the 5th of December, 2021, with the support of the TIS 2B project and the European Agricultural Fund for Rural Development (EAFRD). This work is partially supported by the "SIT feasibility project against *Aedes albopictus* in Réunion Island", TIS 2B (2020-2022), jointly funded by the French Ministry of Health and the European Regional Development Fund (ERDF). YD is (partially) supported by the DST/NRF SARChI Chair in Mathematical Models and Methods in Biosciences and Bioengineering at the University of Pretoria (Grant 82770). YD acknowledges the support of DST/NRF Incentive Grant (Grant 119898). PAB and YD acknowledge the support of the Franco-Columbian program ECOS-Nord (project C17M01), and of the program STIC AmSud (project 20-STIC-05 - NEMBICA). YD acknowledges the support of the Conseil Régional de la Réunion, the Conseil Départemental de la Réunion, the European Agricultural Fund for Rural Development (EAFRD) and the Centre de Coopération Internationale en Recherche Agronomique pour le Développement (CIRAD).

References

[1] B. Adams and M. Boots, *How important is vertical transmission in mosquitoes for the persistence of dengue? Insights from a mathematical model*, Epidemics, 2 (2010), pp. 1 – 10.

[2] R. Anguelov, Y. Dumont, and I. V. Y. Djeumen, *On the use of Traveling Waves for Pest/Vector elimination using the Sterile Insect Technique*, arXiv, 2010.00861 (2020).

[3] M. S. Aronna and Y. Dumont, *On nonlinear pest/vector control via the sterile insect technique: Impact of residual fertility*, Bulletin of Mathematical Biology, 82 (2020), p. 110.

[4] R. Bank, W. Coughran Jr, W. Fichtner, E. Grosse, D. Rose, and R. Smith, *Transient simulation of silicon devices and circuits*, IEEE Trans. Comput.-Aided Design Integr. Circuits Syst., 4 (1985), pp. 436–451.

[5] P.-A. Bliman, D. Cardona-Salgado, Y. Dumont, and O. Vasilieva, *Implementation of control strategies for sterile insect techniques*, Mathematical Biosciences, 314 (2019), pp. 43–60.

[6] J. Bouyer, F. Balestrino, N. Culbert, H. Yamada, and R. Argilés, *Guidelines for Mark-Release-Recapture procedures of Aedes mosquitoes*, FAO/IAEA, 2020, p. 22.

[7] H. Delatte, G. Gimonneau, A. Triboire, and D. Fontenille, *Influence of Temperature on Immature Development, Survival, Longevity, Fecundity, and Gonotrophic Cycles of Aedes albopictus, Vector of Chikungunya and Dengue in the Indian Ocean* , Journal of Medical Entomology, 46 (2009), pp. 33–41.

[8] C. Dufourd and Y. Dumont, *Modeling and Simulations of Mosquito Dispersal. The Case of Aedes albopictus*, Biomath, 1209262 (2012), pp. 1–7.

[9] ——, *Impact of environmental factors on mosquito dispersal in the prospect of sterile insect technique control*, Comput. Math. Appl., 66 (2013), pp. 1695–1715.

[10] Y. Dumont and I. V. Yatat-Djeumen, *Sterile insect technique with accidental releases of sterile females. Impact on mosquito-borne diseases control when viruses are circulating*, Mathematical Biosciences, 343 (2022), p. 108724.

[11] V. A. Dyck, J. Hendrichs, and A. S. Robinson, *The Sterile Insect Technique, Principles and Practice in Area-Wide Integrated Pest Management*, Springer, Dordrecht, 2006.

[12] M. Fried, *Determination of sterile-insect competitiveness*, J. Econ. Entomol., 64 (1971), pp. 869–872.

[13] M. Hosea and L. Shampine, *Analysis and implementation of tr-bdf2*, Appl. Numer. Math., 20 (1996), pp. 21–37.

[14] R. Lacroix, H. Delatte, T. Hue, and P. Reiter, *Dispersal and survival of male and female Aedes albopictus (Diptera: Culicidae) on Réunion Island*, J Med Entomol., 46(5) (2009), pp. 1117–24.

[15] G. Le Goff, D. Damiens, A.-H. Ruttee, L. Payet, C. Lebon, J.-S. Dehecq, and L.-C. Gouagna, *Field evaluation of seasonal trends in relative population sizes and dispersal pattern of Aedes albopictus males in support of the design of a sterile male release strategy*, Parasites & Vectors, 12 (2019), p. 81.

[16] F. Marini, B. Caputo, M. Pombi, G. Tarsitani, and A. della Torre, *Study of Aedes albopictus dispersal in Rome, Italy, using sticky traps in mark-release-recapture experiments.*, Med Vet Entomol., 24(4) (2010).

[17] F. Marini, B. Caputo, M. Pombi, M. Travaglio, F. Montarsi, A. Drago, R. Rosà, M. Manica, and A. Della Torre, *Estimating spatio-temporal dynamics of Aedes albopictus dispersal to guide control interventions in case of exotic arboviruses in temperate regions.*, Scientific Report, 9(1) (2019), p. 10281.

[18] MATLAB, *version 7.14.0.739 (R2012a)*, The MathWorks Inc., Natick, Massachusetts, 2012.

[19] M. C. I. Medeiros, E. C. Boothe, E. B. Roark, and G. L. Hamer, *Dispersal of male and female Culex quinquefasciatus and Aedes albopictus mosquitoes using stable isotope enrichment*, PLOS Neglected Tropical Diseases, 11 (2017), pp. 1–24.

[20] M. A. Natiello and H. G. Solari, *Modelling population dynamics based on experimental trials with genetically modified (ridl) mosquitoes*, Ecological Modelling, 424 (2020), p. 108986.

[21] C. F. Oliva, M. Jacquet, J. Gilles, G. Lemperiere, P.-O. Maquart, S. Quilici, F. Schooneman, M. J. Vreysen, and S. Boyer, *The sterile insect technique for controlling populations of Aedes albopictus (Diptera: Culicidae) on Reunion Island: mating vigour of sterilized males*, PloS one, 7 (2012), p. e49414.

[22] L. Perko, *Differential Equations and Dynamical Systems*, Springer-Verlag, 2006.

[23] S. P. Sinkins, *Wolbachia and cytoplasmic incompatibility in mosquitoes*, Insect Biochemistry and Molecular Biology, 34 (2004), pp. 723 – 729. Molecular and population biology of mosquitoes.

[24] P. van den Driessche, *Reproduction numbers of infectious disease models*, Infectious Disease Modelling, 2 (2017), pp. 288–303.

[25] L. Vavassori, A. Saddler, and P. Müller, *Active dispersal of Aedes albopictus: a mark-release-recapture study using self-marking units*, Parasites & Vectors, 12 (2019).

[26] C. Virgillito, M. Manica, G. Marini, B. Caputo, A. della Torre, and R. Rosà, *Modelling arthropod active dispersal using partial differential equations: the case of the mosquito aedes albopictus*, Ecological Modelling, 456 (2021), p. 109658.

A Appendix

A.1 Proof of Theorem 1

• To show the right inequality in (5a), assume first that

$$\forall t \geqslant 0, \qquad \frac{1}{T}\int_t^{t+T} \Lambda(s)\ ds \leqslant \Lambda_{\text{high}}. \tag{A.1}$$

Then, for any $t \geqslant 0$,

$$\begin{aligned} M_S(t) &= e^{-\mu_S t}M_S(0) + \int_0^t e^{-\mu_S(t-s)}\Lambda(s)\ ds \\ &= e^{-\mu_S t}M_S(0) + \int_0^{t-\lfloor \frac{t}{T}\rfloor T} e^{-\mu_S(t-s)}\Lambda(s)\ ds + \sum_{i=0}^{\lfloor \frac{t}{T}\rfloor -1}\int_{iT}^{(i+1)T} e^{-\mu_S(t-s)}\Lambda(s)\ ds. \end{aligned} \tag{A.2}$$

Due to the fact that $\Lambda \geqslant 0$, the last term is bounded from above by

$$\begin{aligned} \sum_{i=0}^{\lfloor \frac{t}{T}\rfloor -1}\left(\max_{s\in[iT,(i+1)T]} e^{-\mu_S(t-s)}\right)\int_{iT}^{(i+1)T}\Lambda(s)\ ds &\leqslant T\Lambda_{\text{high}}\sum_{i=0}^{\lfloor \frac{t}{T}\rfloor -1} e^{-\mu_S(\lfloor \frac{t}{T}\rfloor -i)T} \\ &= T\Lambda_{\text{high}}\frac{1-e^{-\mu_S\lfloor \frac{t}{T}\rfloor T}}{e^{\mu_S T}-1} \leqslant \frac{T}{e^{\mu_S T}-1}\Lambda_{\text{high}}. \end{aligned}$$

As the first two terms in (A.2) vanishes when $t \to +\infty$, one deduces the rightmost inequality in (5a).
• If (A.1) doesn't hold, then according to the assumptions in the statement, for any $\varepsilon > 0$, there exists $T_\varepsilon \geqslant 0$ such that

$$\forall t \geqslant T_\varepsilon, \qquad \frac{1}{T}\int_t^{t+T}\Lambda(s)\ ds \leqslant \Lambda_{\text{high}} + \varepsilon,$$

and the same argument than below permits to say that, for any $\varepsilon > 0$,

$$\limsup_{t\to+\infty} M_S(t) \leqslant \frac{T}{e^{\mu_S T}-1}(\Lambda_{\text{high}} + \varepsilon).$$

Making $\varepsilon \to 0$ shows that the rightmost inequality in (5a) holds under the assumption of the statement. The demonstration of the leftmost inequality in (5a) is conducted along the same lines.
• The proof of the formulas in (5b) is straightforward, and comes by integration from the inequalities $\dot{M} \geqslant -\mu_M M + m_M$, $\dot{F} \geqslant -\mu_F F + m_F$.
• In order to prove (5c), we first state the following technical result, whose demonstration is postponed to the end of this proof.

Lemma A.1. *For any value $\gamma M_S \geqslant 0$, $\sigma \geqslant 0$, one has*

$$\sup\left\{\frac{FM}{M+\gamma M_S}\ :\ M>0, F\geqslant 0, M+F=\sigma\right\} = \left(\sqrt{\gamma M_S+\sigma}-\sqrt{\gamma M_S}\right)^2 \leqslant \sigma. \tag{A.3}$$

A supremum is put in (A.3) and only positive values of M are considered, in order to avoid any problem of definition of the fraction in the case where $\gamma M_S = 0$.

Let now $\sigma(t) := M(t)+F(t)$. Summing up the first two equations of system (1) and taking advantage of Lemma A.1 and inequality (4), one has

$$\begin{aligned} \dot{\sigma} &= \rho\frac{FM}{M+\gamma M_S}e^{-\beta\sigma} - \min\{\mu_M;\mu_F\}\sigma + m_M^{\text{high}} + m_F^{\text{high}} \\ &\leqslant \left(\rho e^{-\beta\sigma} - \mu_F\right)\sigma + m_M^{\text{high}} + m_F^{\text{high}} \\ &= \left(\rho e^{-\beta\sigma} + \frac{m_M^{\text{high}} + m_F^{\text{high}}}{\sigma} - \mu_F\right)\sigma, \end{aligned}$$

The first factor in the previous expression is a decreasing function of σ on $(0,+\infty)$, with negative limit when $\sigma \to +\infty$. There thus exists a unique

$$\sigma^* := \min\left\{\sigma \geqslant 0 \ : \ \rho e^{-\beta\sigma'} + \frac{m_M^{\rm high} + m_F^{\rm high}}{\sigma'} - \mu_F < 0 \text{ for any } \sigma' > \sigma\right\},$$

and the previous differential inequality implies that, for any trajectory, $M(t) + F(t) = \sigma(t)$ fulfils

$$\limsup_{t\to+\infty}(M(t) + F(t)) \leqslant \sigma^*.$$

This estimate is now improved, as follows, in the case where $\Lambda_{\rm low} > 0$. For any $x \geqslant 0$, one has $\sqrt{1+x} \geqslant 1 + \frac{1}{2}x - \frac{1}{8}x^2$, therefore

$$\begin{aligned}\left(\sqrt{\gamma M_S + \sigma} - \sqrt{\gamma M_S}\right)^2 &= \sigma + 2\gamma M_S - 2\sqrt{\gamma M_S(\gamma M_S + \sigma)} \\ &\leqslant \sigma + 2\gamma M_S\left(1 - \left(1 + \frac{1}{2}\frac{\sigma}{\gamma M_S} - \frac{1}{8}\frac{\sigma^2}{\gamma^2 M_S^2}\right)\right) \\ &= \frac{\sigma^2}{4\gamma M_S} \leqslant \frac{\sigma^{*2}}{4\gamma M_S}.\end{aligned}$$

The previous inequality might be used to study the asymptotic behavior, because $\Lambda_{\rm low} > 0$ implies $0 < \liminf_{t\to+\infty} M_S(t)$, see (5a). Introducing this inequality in (1a), one obtains

$$\dot{M} \leqslant r\rho\frac{\sigma^{*2}}{4\gamma M_S} - \mu_M M + m_M^{\rm high} \leqslant r\rho\frac{\sigma^{*2}\mu_S}{4\gamma\Lambda_{\rm low}} + m_M^{\rm high} - \mu_M M,$$

and thus

$$\limsup_{t\to+\infty} M(t) \leqslant \frac{1}{\mu_M}\left(r\rho\frac{\sigma^{*2}\mu_S}{4\gamma\Lambda_{\rm low}} + m_M^{\rm high}\right),$$

and similarly

$$\limsup_{t\to+\infty} F(t) \leqslant \frac{1}{\mu_F}\left((1-r)\rho\frac{\sigma^{*2}\mu_S}{4\gamma\Lambda_{\rm low}} + m_F^{\rm high}\right).$$

Taking for φ any decreasing function larger or equal than

$$\min\left\{\sigma^*, \frac{1}{\mu_M}\left(r\rho\frac{\sigma^{*2}\mu_S}{4\gamma\Lambda_{\rm low}} + m_M^{\rm high}\right), \frac{1}{\mu_F}\left((1-r)\rho\frac{\sigma^{*2}\mu_S}{4\gamma\Lambda_{\rm low}} + m_F^{\rm high}\right)\right\} \tag{A.4}$$

demonstrates (5c). It now remains to prove Lemma A.1.

Proof of Lemma A.1. Let $M > 0$. The derivative of the map $f \ : \ [0,\sigma] \to \mathbb{R}^+$ defined by

$$f(M) := \frac{M(\sigma - M)}{M + \gamma M_S}$$

is equal to

$$f'(M) := \frac{(\sigma - 2M)(M + \gamma M_S) - M(\sigma - M)}{(M + \gamma M_S)^2} = -\frac{M^2 + 2\gamma M_S M - \sigma\gamma M_S}{(M + \gamma M_S)^2}.$$

It possesses a unique positive zero, namely $\tilde{M} := \sqrt{(\gamma M_S)(\gamma M_S + \sigma)} - \gamma M_S$, so that the optimal, and indeed maximal, value of f on $[0,\sigma]$ is attained at that point, and is equal to

$$\frac{(\sqrt{\gamma M_S(\gamma M_S + \sigma)} - \gamma M_S)(\gamma M_S + \sigma - \sqrt{\gamma M_S(\gamma M_S + \sigma)})}{\sqrt{\gamma M_S(\gamma M_S + \sigma)}} = \left(\sqrt{\gamma M_S + \sigma} - \sqrt{\gamma M_S}\right)^2,$$

that is (A.3). □

With the end of this proof, the demonstration of Theorem 1 is now completed.

A.2 Proofs of Theorems 2 and 3

A.2.1 Proof of Theorem 2

• The equilibrium points are exactly those nonnegative pairs (M^*, F^*) that verify

$$r\rho F^* e^{-\beta(M^*+F^*)} - \mu_M M^* + m_M = 0, \qquad (1-r)\rho F^* e^{-\beta(M^*+F^*)} - \mu_F F^* + m_F = 0 \tag{A.5}$$

In particular, eliminating $F^* e^{-\beta(M^*+F^*)}$ from these two formulas shows that one has necessarily

$$\frac{M^*}{\mathcal{N}_M} - \frac{F^*}{\mathcal{N}_F} = \frac{1}{\mathcal{N}_M}\frac{m_M}{\mu_M} - \frac{1}{\mathcal{N}_F}\frac{m_F}{\mu_F}, \tag{A.6}$$

that is (9b) (or the 2nd part of (8) whenever $m_F = 0$). Introducing the corresponding expression of M^* in the second formula in (A.5) yields equation (9a). It is clear that the nonnegative solutions F^* of (9a) for which identity (9b) yields a nonnegative value M^*, are in one-to-one correspondence with the nonnegative solutions (M^*, F^*) of (A.5), that is to the equilibrium points of (6).
• Consider first the case where $m_F = 0$. There clearly exists a unique solution (M^{**}, F^{**}) of (9a) with $F^{**} = 0$, for which $M^{**} > 0$ is given in the statement.

On the other hand, any positive solution F^* of (9a) fulfils necessarily

$$\exp\left(-\beta\left(1 + \frac{\mathcal{N}_M}{\mathcal{N}_F}\right)F^* - \beta\frac{m_M}{\mu_M}\right) = \frac{1}{\mathcal{N}_F}, \tag{A.7}$$

which yields the first formula in (8). The obtained expression of F^* is positive if and only if (7) holds. In such case, the value of M^* provided by the second formula in (8) is also positive, because $m_M \geqslant 0$.
• Consider now the case where $m_F > 0$. Clearly there exists no equilibrium with $F^* = 0$, so that every equilibrium has to fulfil (9a), that we rewrite here as

$$\Phi(F^*) := \left(\mathcal{N}_F \exp\left(-\beta\left(1 + \frac{\mathcal{N}_M}{\mathcal{N}_F}\right)F^* - \beta\frac{m_M}{\mu_M} + \beta\frac{\mathcal{N}_M}{\mathcal{N}_F}\frac{m_F}{\mu_F}\right) - 1\right)F^* = -\frac{m_F}{\mu_F}. \tag{A.8}$$

The map Φ possesses two roots in $\mathbb{R}$ (possibly identical), namely 0 and the value

$$\frac{1}{1+\frac{\mathcal{N}_M}{\mathcal{N}_F}}\left(\frac{1}{\beta}\log\mathcal{N}_F - \frac{m_M}{\mu_M} + \frac{\mathcal{N}_M}{\mathcal{N}_F}\frac{m_F}{\mu_F}\right),$$

whose sign is undefined. On the other hand, Φ is positive between its roots, and negative otherwise. From this observation, one deduces any positive solution of (A.8) is indeed larger than the largest of the two roots of Φ. In other words, any positive solution pertains indeed to the semi-infinite interval $(h, +\infty)$, where

$$h := \max\left\{0; \frac{1}{1+\frac{\mathcal{N}_M}{\mathcal{N}_F}}\left(\frac{1}{\beta}\log\mathcal{N}_F - \frac{m_M}{\mu_M} + \frac{\mathcal{N}_M}{\mathcal{N}_F}\frac{m_F}{\mu_F}\right)\right\}. \tag{A.9}$$

The function Φ is the product of two terms. *On the interval* $(h, +\infty)$, the first one is a decreasing negative function of F^*, while the linear term is a positive increasing function of F^*: Φ is thus negative and *decreasing* on $(h, +\infty)$, with $\Phi(h) = 0$. As this map is unbounded, (A.8) thus admits a *unique* solution on $(h, +\infty)$.

It now remains to show that the corresponding value M^*, given by (9b), is nonnegative, that is

$$F^* \geqslant -\frac{\mathcal{N}_F}{\mathcal{N}_M}\frac{m_M}{\mu_M} + \frac{m_F}{\mu_F} =: h'. \tag{A.10}$$

Assume first that

$$h' \leqslant h.$$

As necessarily one has $h \leqslant F^*$, one gets directly (A.10).

If on the contrary

$$h' > h \geqslant 0,$$

then, both h' and F^* are located in the interval $[h,+\infty)$ on which Φ is decreasing. In order to prove (A.10), it is thus sufficient to establish that $\Phi(h') \geqslant \Phi(F^*) = -\frac{m_F}{\mu_F}$. One has

$$\Phi(h') = \left(\mathcal{N}_F \exp\left(-\beta\left(1+\frac{\mathcal{N}_M}{\mathcal{N}_F}\right)h' - \beta\frac{m_M}{\mu_M} + \beta\frac{\mathcal{N}_M}{\mathcal{N}_F}\frac{m_F}{\mu_F}\right) - 1\right)h' = \left(\mathcal{N}_F \exp\left(\beta h'\right) - 1\right)h'.$$

Therefore,

$$\Phi(h')+\frac{m_F}{\mu_F} = \left(\mathcal{N}_F \exp\left(\beta h'\right) - 1\right)h'+\frac{m_F}{\mu_F} = \mathcal{N}_F \exp\left(\beta h'\right)h'+\left(\frac{m_F}{\mu_F} - h'\right) = \mathcal{N}_F \exp\left(\beta h'\right)h'+\frac{\mathcal{N}_F}{\mathcal{N}_M}\frac{m_M}{\mu_M}.$$

Both terms of the previous expression are nonnegative, due to the fact that $h' \geqslant 0$. One thus obtained that the unique solution F^* of (A.8) on $[h,+\infty)$ fulfils the inequality (A.10). It thus provides an equilibrium point for (6). As a conclusion, there exists a unique equilibrium point for (6) when $m_F > 0$, as announced in the statement. This achieves the proof of Theorem 2.

A.2.2 Proof of Theorem 3

• Recall for further use that the Jacobian matrix of system (6) is

$$J(M,F) = \begin{pmatrix} -\beta r\rho F e^{-\beta(M+F)} - \mu_M & r\rho(1-\beta F)e^{-\beta(M+F)} \\ -\beta(1-r)\rho F e^{-\beta(M+F)} & (1-r)\rho(1-\beta F)e^{-\beta(M+F)} - \mu_F \end{pmatrix}. \tag{A.11}$$

• Consider first the case $m_F = 0$. The Jacobian matrix at the point $(M^{**},0)$ is the triangular matrix

$$J(M^{**},0) = \begin{pmatrix} -\mu_M & r\rho e^{-\beta M^{**}} \\ 0 & (1-r)\rho e^{-\beta M^{**}} - \mu_F \end{pmatrix},$$

whose local stability follows from the fact that $M^{**} = \dfrac{m_M}{\mu_M}$ and (10), while (7) implies instability. Global asymptotic stability of $(M^{**},0)$ is then straightforward: introducing the change of variable $M \leftarrow M + M^{**}$, we have, for all $F > 0$

$$\dot{F} = (1-r)\rho F e^{-\beta(M+F)-\beta M^{**}} - \mu_F F \leqslant \left(e^{-\beta(M+F)} - 1\right)\mu_F F < 0,$$

thanks to (10) again. We deduce that F is decreasing to 0, and thus that M converges to M^{**}.

Assume now that (7) holds. At the equilibrium (M^*,F^*), (8) yields

$$M^* + F^* = \left(1+\frac{\mathcal{N}_M}{\mathcal{N}_F}\right)F^* + \mathcal{N}_M\tilde{m}_M = \frac{1}{\beta}\left(\log\mathcal{N}_F - \beta\mathcal{N}_M\tilde{m}_M\right) + \mathcal{N}_M\tilde{m}_M = \frac{1}{\beta}\log\mathcal{N}_F,$$

and the Jacobian matrix at this point is equal to

$$J(M^*,F^*) = \begin{pmatrix} -\frac{\beta r\rho}{\mathcal{N}_F}F^* - \mu_M & \frac{r\rho}{\mathcal{N}_F}(1-\beta F^*) \\ -\frac{\beta(1-r)\rho}{\mathcal{N}_F}F^* & \frac{(1-r)\rho}{\mathcal{N}_F}(1-\beta F^*) - \mu_F \end{pmatrix} = \begin{pmatrix} -\frac{\beta r\rho}{\mathcal{N}_F}F^* - \mu_M & \frac{r\rho}{\mathcal{N}_F}(1-\beta F^*) \\ -\frac{\beta(1-r)\rho}{\mathcal{N}_F}F^* & -\frac{\beta(1-r)\rho}{\mathcal{N}_F}F^* \end{pmatrix}.$$

The trace of this matrix is obviously negative, while its determinant is

$$\frac{\beta(1-r)\rho}{\mathcal{N}_F}F^*\left(\mu_M + \frac{r\rho}{\mathcal{N}_F}\right) > 0.$$

The equilibrium (M^*,F^*) is therefore LAS.

In order to show Global Asymptotic Stability of (M^*,F^*), we now apply Dulac criterion. Let

$$\psi_1(F) := \frac{1}{F}, \quad f_1(M,F) := r\rho F e^{-\beta(M+F)} - \mu_M M + m_M, \quad g_1(M,F) := (1-r)\rho F e^{-\beta(M+F)} - \mu_F F + m_F.$$

We study the sign of the function

$$D_1(M,F) := \frac{\partial}{\partial M}\Big(\psi_1(F)f_1(M,F)\Big) + \frac{\partial}{\partial F}\Big(\psi_1(F)g_1(M,F)\Big).$$

We have

$$\frac{\partial}{\partial M}\Big(\psi_1(F)f_1(M,F)\Big) = -\beta r\rho e^{-\beta(M+F)} - \frac{\mu_M}{F},$$
$$\frac{\partial}{\partial F}\Big(\psi_1(F)g_1(M,F)\Big) = -\beta(1-r)\rho e^{-\beta(M+F)} - \frac{m_F}{F^2},$$

and thus

$$D_1(M,F) = -\beta\rho e^{-\beta(M+F)} - \frac{\mu_M}{F} - \frac{m_F}{F^2} < 0$$

for all $(M,F) \in \mathcal{D}$ such that $F > 0$. Therefore, Dulac criterion [22] applies, demonstrating that system (6) possesses no nonconstant periodic solutions when $m_F = 0$. Thus, using the fact that (M^*, F^*) is LAS, by the Poincaré-Bendixson theorem, all trajectories in $\mathcal{D}\backslash\{(M,0) \ : \ M \geqslant 0\}$ converge towards this point.

• Let us now consider the case $m_F > 0$. Thanks to $(A.5)_2$, at equilibrium (M^*, F^*) we have,

$$\mathcal{N}_F F^* e^{-\beta(M^*+F^*)} + \frac{m_F}{\mu_F} = F^*,$$

and we get from the fact that $m_F > 0$, that

$$\mathcal{N}_F F^* e^{-\beta(M^*+F^*)} < F^*.$$

Thus, since $F^* > 0$, we deduce that

$$\mathcal{N}_F e^{-\beta(M^*+F^*)} < 1. \tag{A.12}$$

According to (A.11), we have

$$J^* = J(M^*,F^*) = \begin{pmatrix} -\beta r\rho F^* e^{-\beta(M^*+F^*)} - \mu_M & r\rho(1-\beta F^*)e^{-\beta(M^*+F^*)} \\ -\beta(1-r)\rho F^* e^{-\beta(M^*+F^*)} & (1-r)\rho(1-\beta F^*)e^{-\beta(M^*+F^*)} - \mu_F \end{pmatrix},$$

so that

$$\begin{aligned}
\det(J^*) &= \Big(\beta r\rho F^* e^{-\beta(M^*+F^*)} + \mu_M\Big)\Big(\mu_F - (1-r)\rho(1-\beta F^*)e^{-\beta(M^*++F^*)}\Big) \\
&\quad +\beta(1-r)\rho F^* e^{-\beta(M^*+F^*)} r\rho(1-\beta F^*)e^{-\beta(M^*+F^*)} \\
&= \Big(\beta r\rho F^* e^{-\beta(M^*+F^*)} + \mu_M\Big)\mu_F - \mu_M(1-r)\rho(1-\beta F^*)e^{-\beta(M^*+F^*)} \\
&= \beta r\rho F^* e^{-\beta(M^*+F^*)}\mu_F + \mu_M\mu_F - \mu_F\mu_M\mathcal{N}_F(1-\beta F^*)e^{-\beta(M^*+F^*)} \\
&= \beta r\rho F^* e^{-\beta(M^*+F^*)}\mu_F + \mu_M\mu_F - \mu_F\mu_M\mathcal{N}_F e^{-\beta(M^*+F^*)} + \mu_F\mu_M\mathcal{N}_F\beta F^* e^{-\beta(M^*+F^*)}.
\end{aligned}$$

Then, using (A.12), we deduce that

$$\det(J^*) \geqslant \beta r\rho F^* e^{-\beta(M^*+F^*)}\mu_F + \mu_F\mu_M\mathcal{N}_F\beta F^* e^{-\beta(M^*+F^*)} > 0.$$

In addition, computing the trace $\mathtt{tr}(J^*)$ of J^*, we derive

$$\begin{aligned}
\mathtt{tr}(J^*) &= -\beta r\rho F^* e^{-\beta(M^*+F^*)} - \mu_M + (1-r)\rho(1-\beta F^*)e^{-\beta(M^*+F^*)} - \mu_F \\
&= -\beta\rho F^* e^{-\beta(M^*+F^*)} - \mu_M + (1-r)\rho e^{-\beta(M^*+F^*)} - \mu_F \\
&= -\beta\rho F^* e^{-\beta(M^*+F^*)} - \mu_M + \mu_F\mathcal{N}_F e^{-\beta(M^*+F^*)} - \mu_F < -\beta\rho F^* e^{-\beta(M^*+F^*)} - \mu_M < 0.
\end{aligned}$$

We deduce the Local Asymptotic Stability of (M^*, F^*).

The same argument than in the case $m_F = 0$ above allows to deduce Global Asymptotic Stability from its local counterpart. This achieves the demonstration of Theorem 3.

A.3 Proofs of Lemmas 1 and 2

A.3.1 Proof of Lemma 1

The equilibrium points of (12) are exactly the nonnegative values (M, F) such that

$$\rho F \frac{M}{M+\gamma M_S} e^{-\beta(M+F)} = \frac{1}{r}\left(\mu_M M - m_M\right), \qquad \rho F \frac{M}{M+\gamma M_S} e^{-\beta(M+F)} = \frac{1}{1-r}\left(\mu_F F - m_F\right). \tag{A.13}$$

This yields immediately the necessary conditions

$$M \geqslant \frac{m_M}{\mu_M}, \qquad F \geqslant \frac{m_F}{\mu_F}. \tag{A.14}$$

Eliminating the exponential term in the two formulas in (A.13) yields the following expression for F:

$$F = \frac{1}{\mu_F}\left(\frac{1-r}{r}\left(\mu_M M - m_M\right) + m_F\right) = \frac{\mathcal{N}_F}{\mathcal{N}_M}\left(M - \frac{m_M}{\mu_M}\right) + \frac{m_F}{\mu_F}. \tag{A.15}$$

Inserting now this identity in the first formula in (A.13), we obtain successively the equivalent forms

$$\left(\frac{\mathcal{N}_F}{\mathcal{N}_M}\left(M - \frac{m_M}{\mu_M}\right) + \frac{m_F}{\mu_F}\right) M e^{-\beta\left(M + \frac{\mathcal{N}_F}{\mathcal{N}_M}\left(M - \frac{m_M}{\mu_M}\right) + \frac{m_F}{\mu_F}\right)} = \frac{1}{\rho r}\left(\mu_M M - m_M\right)\left(M + \gamma M_S\right),$$

$$\left(\frac{\mathcal{N}_F}{\mathcal{N}_M}\left(M - \frac{m_M}{\mu_M}\right) + \frac{m_F}{\mu_F}\right) M e^{-\beta\left(M + \frac{\mathcal{N}_F}{\mathcal{N}_M}\left(M - \frac{m_M}{\mu_M}\right) + \frac{m_F}{\mu_F}\right)} = \frac{1}{\mathcal{N}_M}\left(M - \frac{m_M}{\mu_M}\right)\left(M + \gamma M_S\right),$$

$$\left(\mathcal{N}_F\left(M - \frac{m_M}{\mu_M}\right) + \mathcal{N}_M \frac{m_F}{\mu_F}\right) M e^{-\beta\left(M + \frac{\mathcal{N}_F}{\mathcal{N}_M}\left(M - \frac{m_M}{\mu_M}\right) + \frac{m_F}{\mu_F}\right)} = \left(M - \frac{m_M}{\mu_M}\right)\left(M + \gamma M_S\right),$$

that is finally

$$\mathcal{N}_F\left(M - \left(\frac{m_M}{\mu_M} - \frac{m_F}{\mu_F}\frac{\mathcal{N}_M}{\mathcal{N}_F}\right)\right) M e^{-\beta\left(M + \frac{\mathcal{N}_F}{\mathcal{N}_M}\left(M - \left(\frac{m_M}{\mu_M} - \frac{m_F}{\mu_F}\frac{\mathcal{N}_M}{\mathcal{N}_F}\right)\right)\right)} = \left(M - \frac{m_M}{\mu_M}\right)\left(M + \gamma M_S\right).$$

Denoting $x := M$ yields (15), for the constants a, b, c, d, g defined in (13).

Reciprocally, from what was previously established, any nonnegative pair (M, F), where $x = M$ fulfils (15) and F is obtained by (A.15), is an equilibria of (12). As F in (A.15) is nonnegative *if and only if* $M \geqslant c$, while by construction $M \geqslant b \geqslant c$ (see (A.14) and (A.15)), any nonnegative pair (M, F), where $x = M$ fulfils (15) and $x \geqslant b$ is an equilibrium of (12). This achieves the demonstration of Lemma 1.

A.3.2 Proof of Lemma 2

• Let us study the function

$$\Theta \ : \ [b, +\infty) \to \mathbb{R}^+, \qquad x \mapsto \Theta(x) := \frac{(x+a)(x-b)}{x(x-c)} e^{dx}.$$

Observe that $\Theta(b) = 0$ and $\Theta(+\infty) = +\infty$, so that there always exists at least one solution to (20) on $[b, +\infty)$. We are interested in counting the number of minima of Θ, as (20) is equivalent to $\Theta(x) = g$.

The map $x \mapsto \frac{(x+a)(x-b)}{x(x-c)}$ is *not always* increasing on $[b, +\infty)$, so we study the variations of Θ. One has

$$\Theta'(x) \quad = \quad \frac{1}{x^2(x-c)^2}\left[(2x+a-b)x(x-c) - (x+a)(x-b)(2x-c) + d(x+a)(x-b)x(x-c)\right] e^{dx}.$$

With a 4th-order polynomial governing the sign of Θ', positive at $x = b$ and $x = +\infty$, the number of zeros of Θ' in $[b, +\infty)$ may be any number from 0 to 4, and the number of solutions of (20) any number from 1 to 5.

Let us show that in fact, (20) cannot have more than 3 solutions. Let

$$P(x) := (2x + a - b)x(x - c) - (x + a)(x - b)(2x - c) + d(x + a)(x - b)x(x - c).$$

The following identities are true:

$$P(-a) = -a(a + b)(a + c), \quad P(0) = -abc, \quad P(c) = c(a + c)(b - c), \quad P(b) = b(a + b)(b - c). \quad \text{(A.16a)}$$

and, due to the fact that $d > 0$,

$$\lim_{x \to \pm\infty} P(x) = +\infty. \quad \text{(A.16b)}$$

Remind that we consider here the generic case where, on top of (14), we have $b > c$, $b > 0$, and $a > 0$. To summarize,

$$-a < 0 < b, \qquad c < b, \qquad 0 < b.$$

We will now show that the 4th degree polynomial P has at most two zeros on $[b, +\infty)$. For this, consider the two following distinct cases.

- If $c > -a$, then $P(-a) < 0$ and $P(b) > 0$. Due to (A.16b), P has at least one zero on $(-\infty, -a)$, another one on $(-a, b)$, and therefore at most two on $(b, +\infty)$.
- If $c = -a < 0$, then $P(-a) = P(c) = 0$, while $P(b) = b(a + b)^2 > 0$. Let us show that $P'(-a) = 0$. Indeed, when $c = -a$, $P(x) = (2x + a - b)x(x + a) - (x + a)(x - b)(2x + a) + d(x + a)^2(x - b)$. The last term has zero derivative at $x = -a$, while the sum of the two first terms is $(x + a)((2x + a - b)x - (x - b)(2x + a))$, i.e. $b(x + a)^2$, whose derivative also vanishes at $x = -a$. Due to the existence of a double root at this point, P has at most two zeros on $(b, +\infty)$.

Therefore the polynomial P, and thus the map Θ', possess at most two zeros on $(b, +\infty)$. One deduces that the equation $\Theta(x) = g$ possesses at most three solutions on $(b, +\infty)$, which is the point 1. of Lemma 2.

• To establish the point 2. , let us now study the dependance with respect to the parameter a. For this, we write more explicitly

$$\Theta_a(x) := \Theta(x) = \frac{(x + a)(x - b)}{x(x - c)} e^{dx}.$$

Let $0 < a < a'$. One then has

$$\Theta_{a'}(x) - \Theta_a(x) = (a' - a)\Delta(x), \qquad \Delta(x) := \frac{(x - b)}{x(x - c)} e^{dx},$$

where $\Delta(x) > 0$ for any $x > b$. Let $x^* > b$ be the largest solution of (20) for the value a. By definition, $\Theta_a(x^*) = g$, and $\Theta_a(x) > g$ for any $x \in (x^*, +\infty)$. Due to the fact that $a' > a$, one then has $\Theta_{a'}(x) > g$ for any $x \in (x^*, +\infty)$. This implies that all solutions of the equation $\Theta_{a'}(x) = g$ are smaller than a, including the largest one. We deduce that the largest solution of the equation $\Theta_a(x) = g$ is a decreasing function of a.

Also, due to the fact that $\Delta(x) \to +\infty$ when $x \to +\infty$ (as $d > 0$), one has, for any $\varepsilon > 0$, $\min\{\Delta(x) : x > b + \varepsilon\} > 0$. Using this property, one sees that the largest solution of the equation $\Theta_a(x) = g$ converges to b^+ when $a \to +\infty$.

• Let us now demonstrate the point 3. One may see straightforwardly that, for Δ defined above,

$$\Delta'(b) = \frac{e^{db}}{b(b - c)} > 0.$$

One has, say, $\Theta_a(x) = \Theta_0(x) + a\Delta(x)$. Due to the fact that $\Delta'(b) > 0$, for the large values of a, $\Theta_a(x)$ is not only positive, but also increasing, in an interval right of b. Consequently, for large enough values of a, there is only one solution to the equation $\Theta_a(x) = g$ in the interval $[b, +\infty)$. This demonstrates the point 3. and achieves the proof of Lemma 2.

A.4 Proof of Theorem 6

• 1. Notice that, for any $M, F \geqslant 0$ and any $t \geqslant 0$,

$$\frac{M}{M+\gamma M_S^{\rm per}} e^{-\beta(M+F)} \leqslant \frac{M}{M+\gamma M_S^{\rm per}} e^{-\beta M} \leqslant \frac{1}{e\beta} \frac{1}{M+\gamma M_S^{\rm per}} \leqslant \frac{1}{e\beta\gamma} \frac{1}{M_S^{\rm per}},$$

where we used the fact that $\max\left\{xe^{-\beta x} \ : \ x \geqslant 0\right\} = \frac{1}{e\beta}$. Therefore one deduces from (22b) that

$$\dot{F} \leqslant \left((1-r)\rho \frac{1}{e\beta\gamma} \frac{1}{M_S^{\rm per}} - \mu_F \right) F + m_F^{\rm high}.$$

Let us now state the following technical result.

Lemma A.2. *Let x be a solution of the differential inequality*

$$\dot{x} \leqslant a(t)x + b, \tag{A.17}$$

for a nonnegative *number b and a τ-*periodic *function a such that*

$$I := \int_0^\tau a(t)\, dt < 0. \tag{A.18}$$

Then,

$$\limsup_{t\to+\infty} x(t) \leqslant b\, \Psi[a], \tag{A.19a}$$

where

$$\begin{aligned} \Psi[a] \ &:= \ (1 - e^{\int_0^\tau a(t)\, dt})^{-1} \max_{t\in[0,\tau]} \int_0^\tau e^{\int_{t+s}^{t+\tau} a(\sigma)\, d\sigma}\, ds \\ &= \ -\frac{1}{\max\left\{ a(t) \ : \ t\in[0,\tau),\ a(t)\int_0^\tau e^{\int_{t+s}^{t+\tau} a(\sigma)\, d\sigma}\, ds = e^I - 1 \right\}}. \end{aligned} \tag{A.19b}$$

Notice that the denominator of (A.19b) is negative, so that the right-hand side is positive.

Provided that

$$(1-r)\rho \frac{1}{e\beta\gamma} \left\langle \frac{1}{M_S^{\rm per}} \right\rangle < \mu_F,$$

that is

$$\left\langle \frac{1}{M_S^{\rm per}} \right\rangle < e\beta\gamma \frac{1}{\mathcal{N}_F}, \tag{A.20}$$

one has, by use of Lemma A.2:

$$\limsup_{t\to+\infty} F(t) \leqslant \Psi\left[(1-r)\rho \frac{1}{e\beta\gamma} \frac{1}{M_S^{\rm per}} - \mu_F \right] m_F^{\rm high}, \tag{A.21a}$$

for the function Ψ defined in (A.19b).

Incidentally, due to Lemma A.2, there exists a time instant $t^* \in [0, T)$ such that

$$\Psi\left[(1-r)\rho \frac{1}{e\beta\gamma} \frac{1}{M_S^{\rm per}} - \mu_F \right] = \frac{1}{\mu_F - (1-r)\rho \frac{1}{e\beta\gamma} \frac{1}{M_S^{\rm per}(t^*)}},$$

and this permits to verify that

$$\frac{m_F^{\rm high}}{\mu_F - (1-r)\rho \frac{1}{e\beta\gamma} \frac{1}{M_S^{\rm per}(t^*)}} \geqslant \frac{m_F^{\rm high}}{\mu_F}.$$

From (22a), one now obtains that

$$\limsup_{t\to+\infty}(\dot{M}+\mu_M M) \leqslant r\rho m_F^{\text{high}}\Psi\left[(1-r)\rho\frac{1}{e\beta\gamma}\frac{1}{M_S^{\text{per}}}-\mu_F\right]+m_M^{\text{high}},$$

so that finally

$$\limsup_{t\to+\infty} M(t) \leqslant \frac{1}{\mu_M}m_M^{\text{high}}+\mathcal{N}_M\Psi\left[(1-r)\rho\frac{1}{e\beta\gamma}\frac{1}{M_S^{\text{per}}}-\mu_F\right]m_F^{\text{high}}. \tag{A.21b}$$

Notice that this value is clearly at most equal to $\dfrac{1}{\mu_M}m_M^{\text{high}}$.

To establish (A.21), it remains to show Lemma A.2.

Proof of Lemma A.2. The case where $b=0$ is obtained straightforwardly. To tackle the case $b>0$, we assume in the sequel with no loss of generality that $b=1$ (otherwise argue on $\frac{1}{b}x$).
• First, any trajectory of (1) is bounded from above on $[0,+\infty)$ by the solution of the differential equation

$$\dot{y} = a(t)y+1 \tag{A.22}$$

such that $y(0)=x(0)$. Therefore, using comparison principle, it is sufficient to establish (A.19a) for any solution y of (A.22).
• Equation (A.22) admits a unique τ-periodic solution. As a matter of fact, any solution fulfils

$$(\dot{y}-a(t)y)\,e^{-\int_0^t a(\sigma)\,d\sigma} = e^{-\int_0^t a(\sigma)\,d\sigma}.$$

Thanks to (A.18), one has by integration over any interval $(t,t+\tau)$:

$$y(t+\tau)=y(t)e^{\int_t^{t+\tau}a(\sigma)\,d\sigma}+\int_t^{t+\tau}e^{\int_s^{t+\tau}a(\sigma)\,d\sigma}\,ds = y(t)e^I+\int_t^{t+\tau}e^{\int_s^{t+\tau}a(\sigma)\,d\sigma}\,ds = y(t)e^I+\int_0^{\tau}e^{\int_{t+s}^{t+\tau}a(\sigma)\,d\sigma}\,ds.$$

One has used first the fact that, due to the τ-periodicity of a, the map $t\mapsto e^{\int_t^{t+\tau}a(\sigma)\,d\sigma}$ is constant; and a change of variables to modify the second term.

Therefore, necessarily any τ-periodic solution y_τ of (A.22) fulfils

$$y_\tau(t) = (1-e^I)^{-1}\int_0^\tau e^{\int_{t+s}^{t+\tau}a(\sigma)\,d\sigma}\,ds = \Psi[a]. \tag{A.23}$$

Reciprocally, it is straightfoward to show that the previous formula defines a τ-periodic solution of (A.22). Notice that (A.19a) holds for y_τ defined in (A.23).
• We now show that the τ-periodic function y_τ defined in (A.23) attracts all solutions of (7). Let y be any solution of (7), then, by linearity, one has

$$\dot{y}-\dot{y}_\tau = a(t)(y-y_\tau),$$

so that

$$y(t)-y_\tau(t) = e^{\int_0^t a(\sigma)\,d\sigma}(y(0)-y_\tau(0)),$$

which vanishes when $t\to\infty$, due to (A.18). The periodic trajectory y_τ is thus globally asymptotically stable.
• From the fact that (A.19a) holds for y_τ, together with the global asymptotic stability of this solution, one deduces that this property holds indeed for any solution y of (A.22), and finally for any solution x of inequality (A.17).
• It remains to show the equality between the two expressions in (A.19b).

The map $t\mapsto\int_0^\tau e^{\int_{t+s}^{t+\tau}a(\sigma)\,d\sigma}\,ds$ that appears in the definition of Ψ is evidently τ-periodic. To find its maximal value, notice that its derivative vanishes whenever

$$\int_0^\tau (a(t+\tau)-a(t+s))\,e^{\int_{t+s}^{t+\tau}a(\sigma)\,d\sigma}\,ds = 0,$$

that is

$$a(t)\int_0^\tau e^{\int_{t+s}^{t+\tau} a(\sigma)\,d\sigma}\,ds = a(t+\tau)\int_0^\tau e^{\int_{t+s}^{t+\tau} a(\sigma)\,d\sigma}\,ds = \int_0^\tau a(t+s)e^{\int_{t+s}^{t+\tau} a(\sigma)\,d\sigma}\,ds = \Big[-e^{\int_{t+s}^{t+\tau} a(\sigma)\,d\sigma}\Big]_{s=0}^{s=\tau} = e^I - 1.$$

Therefore,

$$\int_0^\tau e^{\int_{t+s}^{t+\tau} a(\sigma)\,d\sigma}\,ds = \frac{e^I-1}{a(t)}$$

at any point where $\int_0^\tau e^{\int_{t+s}^{t+\tau} a(\sigma)\,d\sigma}\,ds$ is extremal, and reciprocally this identity holds only at points where the derivative of the map $t \mapsto \int_0^\tau e^{\int_{t+s}^{t+\tau} a(\sigma)\,d\sigma}\,ds$ vanishes. Inserting this expression in the definition of Ψ yields:

$$\begin{aligned}\Psi[a] &= \max\left\{-\frac{1}{a(t)}\ :\ t\in[0,\tau),\ a(t)\int_0^\tau e^{\int_{t+s}^{t+\tau} a(\sigma)\,d\sigma}\,ds = e^I-1\right\}\\ &= -\frac{1}{\max\left\{a(t)\ :\ t\in[0,\tau),\ a(t)\int_0^\tau e^{\int_{t+s}^{t+\tau} a(\sigma)\,d\sigma}\,ds = e^I-1\right\}},\end{aligned}$$

which is (A.19b) when $b=1$. This achieves the demonstration of Lemma A.2. □

• 2. We now proceed with the proof of Theorem 6. The same argument may be conducted from (22a) rather than (22b), leading to the estimate:

$$\frac{F}{M+\gamma M_S^{\rm per}}e^{-\beta(M+F)} \leqslant \frac{1}{e\beta\gamma M_S^{\rm per}}.$$

If

$$\left\langle \frac{1}{M_S^{\rm per}} \right\rangle < e\beta\gamma\frac{1}{\mathcal{N}_M}, \tag{A.24}$$

one then has

$$\limsup_{t\to+\infty} M(t) \leqslant \Psi\left[r\rho\frac{1}{e\beta\gamma}\frac{1}{M_S^{\rm per}} - \mu_M\right] m_M^{\rm high}. \tag{A.25a}$$

It may then be shown as before that the coefficient of $m_M^{\rm high}$ is at least equal to $\frac{1}{\mu_M}$.

From (22b), one then gets

$$\limsup_{t\to+\infty} F(t) \leqslant \mathcal{N}_F\Psi\left[r\rho\frac{1}{e\beta\gamma}\frac{1}{M_S^{\rm per}} - \mu_M\right] m_M^{\rm high} + \frac{1}{\mu_F}m_F^{\rm high}. \tag{A.25b}$$

• 3. We now introduce a third and last estimate. Define the positive definite function

$$\mathcal{V}(M,F) := \frac{1}{2}(M^2+F^2). \tag{A.26}$$

Its derivative along the trajectories of (22) fulfils

$$\dot{\mathcal{V}} = M\dot{M} + F\dot{F} \leqslant -\mu_M M^2 - \mu_F F^2 + \rho\frac{FM(rM+(1-r)F)}{M+\gamma M_S^{\rm per}}e^{-\beta(M+F)} + m_M^{\rm high}M + m_F^{\rm high}F. \tag{A.27}$$

On the one hand, we have

$$-\mu_M M^2 - \mu_F F^2 \leqslant -\min\{\mu_M,\mu_F\}(M^2+F^2) = -2\min\{\mu_M,\mu_F\}\mathcal{V}.$$

On the other hand,

$$\begin{aligned}\frac{FM(rM+(1-r)F)}{M+\gamma M_S^{\rm per}}e^{-\beta(M+F)} &\leqslant \max\{r,1-r\}\frac{FM(M+F)}{M+\gamma M_S^{\rm per}}e^{-\beta(M+F)}\\ &\leqslant \max\{r,1-r\}\frac{1}{e\beta}\frac{FM}{M+\gamma M_S^{\rm per}}\\ &\leqslant \max\{r,1-r\}\frac{1}{e\beta}\frac{1}{M+\gamma M_S^{\rm per}}\mathcal{V}\\ &\leqslant \max\{r,1-r\}\frac{1}{e\beta\gamma}\frac{1}{M_S^{\rm per}}\mathcal{V}.\end{aligned}$$

Coming back to (A.27), we deduce that

$$\dot{\mathcal{V}} \leqslant \left(\max\{r, 1-r\} \frac{1}{e\beta\gamma M_S^{\rm per}} - 2\min\{\mu_M, \mu_F\} \right) \mathcal{V} + 2\max\{m_M^{\rm high}, m_F^{\rm high}\}\, \mathcal{V}^{1/2},$$

that is

$$\frac{1}{2}\frac{d\mathcal{V}^{1/2}}{dt} \leqslant \left(\max\{r, 1-r\} \frac{1}{e\beta\gamma M_S^{\rm per}} - 2\min\{\mu_M, \mu_F\} \right) \mathcal{V}^{1/2} + 2\max\{m_M^{\rm high}, m_F^{\rm high}\}.$$

Using again Lemma A.2, provided that

$$\max\{r, 1-r\}\rho \frac{1}{e\beta\gamma} \left\langle \frac{1}{M_S^{\rm per}} \right\rangle < 2\min\{\mu_M, \mu_F\},$$

that is,

$$\left\langle \frac{1}{M_S^{\rm per}} \right\rangle < 2e\beta\gamma \frac{\min\{\mu_M, \mu_F\}}{\max\{r, 1-r\}\rho} = 2e\beta\gamma \frac{1}{\max\{r, 1-r\}} \min\left\{ \frac{r}{\mathcal{N}_{\mathcal{M}}}, \frac{1-r}{\mathcal{N}_F} \right\}, \tag{A.28}$$

one gets that the function $\mathcal{V}^{1/2} = (M^2 + F^2)^{1/2}$ fulfils

$$\limsup_{t \to +\infty} \mathcal{V}^{1/2}(t) \leqslant 4\Psi \left[2 \left(\max\{r, 1-r\} \frac{1}{e\beta\gamma M_S^{\rm per}} - 2\min\{\mu_M, \mu_F\} \right) \right] \max\{m_M^{\rm high}, m_F^{\rm high}\}. \tag{A.29}$$

• 4. Putting together the sufficient conditions in (A.20), (A.24) and (A.28) yields the following sufficient condition for existence of an inequality of type (24):

$$\left\langle \frac{1}{M_S^{\rm per}} \right\rangle \quad < \quad e\beta\gamma \max\left\{ \frac{1}{\mathcal{N}_M}, \frac{1}{\mathcal{N}_F}, \frac{2}{\max\{r, 1-r\}} \min\left\{ \frac{r}{\mathcal{N}_M}, \frac{1-r}{\mathcal{N}_F} \right\} \right\}.$$

Arguing as in [5, Proof of Theorem 5], one expresses the mean value of $\dfrac{1}{M_S^{\rm per}}$ as a function of Λ, and transforms the previous inequality to get formula (23).

• 5. Last, for large enough Λ, each one of the three estimates may be used. Consider e.g. (A.21). As $\dfrac{1}{M_S^{\rm per}}$ converges to 0 when $\Lambda \to +\infty$, one deduces the formulas in (25), by invoking continuity of Ψ (relatively to the uniform convergence). This concludes the proof of Theorem 6.

A.5 Proofs of Proposition 7, Lemma 3, Theorems 9 and 10

A.5.1 Proof of Proposition 7

Applying condition (27) to (1) yields the following differential inequalities on $(0, +\infty)$:

$$\dot{M} = r\rho \frac{FM}{M + \gamma M_S} e^{-\beta(M+F)} - \mu_M M + m_M(t) \leqslant r\rho \frac{FM}{M + \gamma M_S} - \mu_M M + m_M^{\rm high} \leqslant -\mu_M M + r\rho k F + m_M^{\rm high}$$

and

$$\dot{F} = (1-r)\rho \frac{FM}{M + \gamma M_S} e^{-\beta(M+F)} - \mu_F F + m_F(t) \leqslant ((1-r)\rho k - \mu_F) F + m_F^{\rm high}.$$

The linear, non-homogeneous, autonomous system

$$\begin{pmatrix} \dot{M}' \\ \dot{F}' \end{pmatrix} = \begin{pmatrix} -\mu_M & r\rho k \\ 0 & -\mu_F + (1-r)\rho k \end{pmatrix} \begin{pmatrix} M' \\ F' \end{pmatrix} + \begin{pmatrix} m_M^{\rm high} \\ m_F^{\rm high} \end{pmatrix}, \qquad t \geqslant 0 \tag{A.30}$$

involves a Metzler matrix, and is thus monotone. As such, it may serve as a comparison system for the evolution of (1), yielding

$$0 \leqslant M(t) \leqslant M'(t), \qquad 0 \leqslant F(t) \leqslant F'(t), \qquad t \geqslant 0,$$

where (M', F') is the solution of (A.30) generated by the same initial values as the underlying solution (M, F) of (1).

For $k < \frac{1}{\mathcal{N}_F}$, $-\mu_F + (1-r)\rho k < 0$, so that the linear system (A.30) is asymptotically stable, yielding:

$$\begin{aligned}\limsup_{t\to+\infty}\begin{pmatrix}M(t)\\F(t)\end{pmatrix} &\leqslant \lim_{t\to+\infty}\begin{pmatrix}M'(t)\\F'(t)\end{pmatrix}\\ &= -\begin{pmatrix}-\mu_M & r\rho k\\ 0 & -\mu_F+(1-r)\rho k\end{pmatrix}^{-1}\begin{pmatrix}m_M^{\text{high}}\\ m_F^{\text{high}}\end{pmatrix}\\ &= \frac{1}{\mu_M(\mu_F-(1-r)\rho k)}\begin{pmatrix}\mu_F-(1-r)\rho k & r\rho k\\ 0 & \mu_M\end{pmatrix}\begin{pmatrix}m_M^{\text{high}}\\ m_F^{\text{high}}\end{pmatrix},\end{aligned}$$

and the formulas in (28). This achieves the proof of Proposition 7.

A.5.2 Proof of Lemma 3

Using superposition principle, write $M' = M'_1 + M'_2$, $F' = F'_1 + F'_2$, where

$$\begin{pmatrix}\dot{M}'_1\\ \dot{F}'_1\end{pmatrix} = \begin{pmatrix}-\mu_M & r\rho k\\ 0 & -\mu_F+(1-r)\rho k\end{pmatrix}\begin{pmatrix}M'_1\\ F'_1\end{pmatrix}, \qquad \begin{pmatrix}M'_1(0)\\ F'_1(0)\end{pmatrix} = \begin{pmatrix}M(n\tau)\\ F(n\tau)\end{pmatrix}$$
$$\begin{pmatrix}\dot{M}'_2\\ \dot{F}'_2\end{pmatrix} = \begin{pmatrix}-\mu_M & r\rho k\\ 0 & -\mu_F+(1-r)\rho k\end{pmatrix}\begin{pmatrix}M'_2\\ F'_2\end{pmatrix} + \begin{pmatrix}m_M^{\text{high}}\\ m_F^{\text{high}}\end{pmatrix}, \qquad \begin{pmatrix}M'_2(0)\\ F'_2(0)\end{pmatrix} = \begin{pmatrix}0\\0\end{pmatrix}.$$

One then checks easily that, for any $t \in (n\tau, (n+1)\tau]$,

$$\begin{pmatrix}M'_1(t)\\ F'_1(t)\end{pmatrix} = P(t-n\tau)\begin{pmatrix}M(n\tau)\\ F(n\tau)\end{pmatrix}, \qquad \begin{pmatrix}M'_2(t)\\ F'_2(t)\end{pmatrix} = Q(t-n\tau)\begin{pmatrix}m_M^{\text{high}}\\ m_F^{\text{high}}\end{pmatrix},$$

for

$$P(t) := \exp\left(\begin{pmatrix}-\mu_M & r\rho k\\ 0 & -\mu_F+(1-r)\rho k\end{pmatrix}t\right) \tag{A.31a}$$

$$Q(t) := \int_0^t P(s)\,ds = \begin{pmatrix}-\mu_M & r\rho k\\ 0 & -\mu_F+(1-r)\rho k\end{pmatrix}^{-1}(P(t)-I_2). \tag{A.31b}$$

The formulas in the statement of Lemma 3 are then obtained directly by application of the following result.

Lemma A.3. *For real scalars a, b, c with $a, b \neq 0$, let*

$$N := \begin{pmatrix}a & c\\ 0 & b\end{pmatrix} \in \mathbb{R}^{2\times 2}.$$

Then, denoting $I_2 \in \mathbb{R}^{2\times 2}$ the identity matrix, one has, for any real number t,

$$e^{Nt} = \begin{pmatrix}e^{at} & \frac{c}{a-b}(e^{at}-e^{bt})\\ 0 & e^{bt}\end{pmatrix} = e^{at}\begin{pmatrix}1 & \frac{c}{a-b}\\ 0 & 0\end{pmatrix} + e^{bt}\begin{pmatrix}0 & -\frac{c}{a-b}\\ 0 & 1\end{pmatrix} \tag{A.32a}$$

$$N^{-1}(e^{Nt}-I_2) = \frac{1}{a}(e^{at}-1)\begin{pmatrix}1 & \frac{c}{a-b}\\ 0 & 0\end{pmatrix} + \frac{1}{b}(e^{bt}-1)\begin{pmatrix}0 & -\frac{c}{a-b}\\ 0 & 1\end{pmatrix} \tag{A.32b}$$

Proof. One checks directly that the expression provided for e^{Nt} in (A.32a) is equal to I_2 for $t = 0$, and is such that

$$\frac{d}{dt}e^{Nt} = Ne^{Nt}.$$

Formula (A.32b) is then obtained straightforwardly, noticing that

$$N^{-1}(e^{Nt}-I_2) = \int_0^t N(s)\,ds,$$

and achieving termwise integration of the right-hand side. This proves Lemma A.3. □

A.5.3 Proof of Theorem 9

The estimate (28) holds, therefore when equality is taken in (32a), there exists $\Lambda^{\rm feed} > 0$ for which the uniform estimate in (33) holds. Moreover, one deduces from (31) that

$$\begin{aligned}
\tau\Lambda_n &\leqslant \frac{1}{\gamma}\left(\frac{1}{k}-1\right)\begin{pmatrix}1 & 0\end{pmatrix}\left(P(\tau)\begin{pmatrix}M(n\tau)\\ F(n\tau)\end{pmatrix}+Q(\tau)\begin{pmatrix}m_M^{\rm high}\\ m_F^{\rm high}\end{pmatrix}\right)\\
&\leqslant \frac{1}{\gamma}\left(\frac{1}{k}-1\right)\begin{pmatrix}1 & 0\end{pmatrix}\left(P(\tau)\begin{pmatrix}\mu_M & -r\rho k\\ 0 & \mu_F-(1-r)\rho k\end{pmatrix}^{-1}+Q(\tau)\right)\begin{pmatrix}m_M^{\rm high}\\ m_F^{\rm high}\end{pmatrix}\\
&= \frac{1}{\gamma}\left(\frac{1}{k}-1\right)\begin{pmatrix}1 & 0\end{pmatrix}\begin{pmatrix}\mu_M & -r\rho k\\ 0 & \mu_F-(1-r)\rho k\end{pmatrix}^{-1}\begin{pmatrix}m_M^{\rm high}\\ m_F^{\rm high}\end{pmatrix}\qquad\text{(by use of (A.31b))}\\
&= \frac{1}{\gamma}\left(\frac{1}{k}-1\right)\frac{1}{\mu_M}\begin{pmatrix}1 & \frac{r\rho k}{\mu_F-(1-r)\rho k}\end{pmatrix}\begin{pmatrix}m_M^{\rm high}\\ m_F^{\rm high}\end{pmatrix}
\end{aligned}$$

which gives the value of $\Lambda^{\rm feed}$ expressed in formula (33).

A.5.4 Proof of Theorem 10

Let us establish that, under the hypotheses of the statement, one has for every $n \in \mathbb{N}$,

$$\gamma M_S(t) \geqslant \left(\frac{1}{k}-1\right)M'(t), \qquad t \in (np\tau,(n+1)p\tau], \tag{A.33}$$

where M' is the solution of (30) initialized according to $\big(M'(n\tau),F'(n\tau)\big)=\big(M(n\tau),F(n\tau)\big)$.

Let us first evaluate the value of M_S on the interval $(np\tau,(n+1)p\tau]$ of length $p\tau$, at a date $t = s+(np+m)\tau$, where $m \in \{0,1,\dots,p-1\}$ and $s \in (0,\tau]$. Here, $np\tau$ represents the date where the last measurement was achieved, and $(np+m)\tau$ the date of the last release. The value of $M_S(s+(np+m)\tau)$ is given by:

$$\begin{aligned}
M_S\big(s+(np+m)\tau\big) &= \Big(\Lambda_{np+m}\tau + M_S\big((np+m)\tau\big)\Big)e^{-\mu_S s}\\
&= \Big(\Lambda_{np+m}\tau+\Lambda_{np+m-1}\tau e^{-\mu_S\tau}+\cdots+\Lambda_{np}\tau e^{-m\mu_S\tau}+M_S(np\tau)e^{-m\mu_S\tau}\Big)e^{-\mu_S s}.
\end{aligned}$$

On the other hand, using a formula analogous to (30a), one finds that at time $t = s+(np+m)\tau$,

$$\begin{aligned}
M'(s+(np+m)\tau) &= \begin{pmatrix}1 & 1\end{pmatrix}\begin{pmatrix}M'(s+(np+m)\tau)\\ F'(s+(np+m)\tau)\end{pmatrix}\\
&= \begin{pmatrix}1 & 1\end{pmatrix}\left(P(s+m\tau)\begin{pmatrix}M(np\tau)\\ F(np\tau)\end{pmatrix}+Q(s+m\tau)\begin{pmatrix}m_M^{\rm high}\\ m_F^{\rm high}\end{pmatrix}\right)\\
&= \begin{pmatrix}e^{-\mu_M(s+m\tau)} & \dfrac{r\rho k}{\mu_M-\mu_F+(1-r)\rho k}\left(e^{-(\mu_F-(1-r)\rho k)(s+m\tau)}-e^{-\mu_M(s+m\tau)}\right)\end{pmatrix}\begin{pmatrix}M(np\tau)\\ F(np\tau)\end{pmatrix}\\
&\quad+\begin{pmatrix}\frac{1-e^{-\mu_M(s+m\tau)}}{\mu_M} & \dfrac{r\rho k}{\mu_M-\mu_F+(1-r)\rho k}\left(\frac{1-e^{-(\mu_F-(1-r)\rho k)(s+m\tau)}}{\mu_F-(1-r)\rho k}-\frac{1-e^{-\mu_M(s+m\tau)}}{\mu_M}\right)\end{pmatrix}\begin{pmatrix}m_M^{\rm high}\\ m_F^{\rm high}\end{pmatrix}
\end{aligned}$$

Inequality (A.33) is thus fulfilled on $(np\tau,(n+1)p\tau]$ *iff* for any $m \in \{0,1,\dots,p-1\}$ and $s \in (0,\tau]$,

$$\begin{aligned}
&\gamma\Big(\Lambda_{np+m}\tau+\Lambda_{np+m-1}\tau e^{-\mu_S\tau}+\cdots+\Lambda_{np}\tau e^{-m\mu_S\tau}+M_S(np\tau)e^{-m\mu_S\tau}\Big)e^{-\mu_S s}\\
&\geqslant \left(\frac{1}{k}-1\right)\left[\begin{pmatrix}e^{-\mu_M(s+m\tau)} & \dfrac{r\rho k}{\mu_M-\mu_F+(1-r)\rho k}\left(e^{-(\mu_F-(1-r)\rho k)(s+m\tau)}-e^{-\mu_M(s+m\tau)}\right)\end{pmatrix}\begin{pmatrix}M(np\tau)\\ F(np\tau)\end{pmatrix}\right.\\
&\quad\left.+\begin{pmatrix}\frac{1-e^{-\mu_M(s+m\tau)}}{\mu_M} & \dfrac{r\rho k}{\mu_M-\mu_F+(1-r)\rho k}\left(\frac{1-e^{-(\mu_F-(1-r)\rho k)(s+m\tau)}}{\mu_F-(1-r)\rho k}-\frac{1-e^{-\mu_M(s+m\tau)}}{\mu_M}\right)\end{pmatrix}\begin{pmatrix}m_M^{\rm high}\\ m_F^{\rm high}\end{pmatrix}\right],
\end{aligned}$$

that is:

$$\begin{aligned}
&\Lambda_{np+m}\tau e^{m\mu_S\tau} + \Lambda_{np+m-1}\tau e^{(m-1)\mu_S\tau} + \cdots + \Lambda_{np}\tau + M_S(np\tau) \\
&\geqslant \frac{1}{\gamma}\left(\frac{1}{k} - 1\right) e^{\mu_S(s+m\tau)} \times \\
&\quad \left[\begin{pmatrix} e^{-\mu_M(s+m\tau)} & \dfrac{r\rho k}{\mu_M - \mu_F + (1-r)\rho k}\left(e^{-(\mu_F-(1-r)\rho k)(s+m\tau)} - e^{-\mu_M(s+m\tau)}\right) \end{pmatrix} \begin{pmatrix} M(np\tau) \\ F(np\tau) \end{pmatrix}\right. \\
&\quad \left. + \begin{pmatrix} \frac{1-e^{-\mu_M(s+m\tau)}}{\mu_M} & \dfrac{r\rho k}{\mu_M - \mu_F + (1-r)\rho k}\left(\frac{1-e^{-(\mu_F-(1-r)\rho k)(s+m\tau)}}{\mu_F-(1-r)\rho k} - \frac{1-e^{-\mu_M(s+m\tau)}}{\mu_M}\right) \end{pmatrix} \begin{pmatrix} m_M^{\text{high}} \\ m_F^{\text{high}} \end{pmatrix}\right].
\end{aligned}$$

From the fact that

$$\mu_F - (1-r)\rho k \leqslant \mu_F \leqslant \mu_M \leqslant \mu_S,$$

one deduces that the right-hand side of the previous formula is increasing with respect to s. Therefore, it is fulfilled for any $s \in (0, \tau]$ *iff* it is fulfilled for $s = \tau$; that is *iff*

$$\begin{aligned}
\Lambda_{np+m}\tau \quad \geqslant \quad & -M_S(np\tau)e^{-m\mu_S\tau} - \sum_{i=0}^{m-1} \Lambda_{np+i}\tau e^{-(m-i)\mu_S\tau} + \frac{e^{\mu_S\tau}}{\gamma} \times \\
& \left[\frac{1-k}{k} e^{-\mu_M(m+1)\tau} M(np\tau)\right. \\
& + \frac{r\rho(1-k)}{\mu_M - \mu_F + (1-r)\rho k}\left(e^{-(\mu_F-(1-r)\rho k)(m+1)\tau} - e^{-\mu_M(m+1)\tau}\right) F(np\tau) \\
& + \frac{1-k}{k}\frac{1-e^{-\mu_M(m+1)\tau}}{\mu_M} m_M^{\text{high}} \\
& \left. + \frac{r\rho(1-k)}{\mu_M - \mu_F + (1-r)\rho k}\left(\frac{1-e^{-(\mu_F-(1-r)\rho k)(m+1)\tau}}{\mu_F - (1-r)\rho k} - \frac{1-e^{-\mu_M(m+1)\tau}}{\mu_M}\right) m_F^{\text{high}}\right]
\end{aligned}$$

holds. One recognizes condition (37). The proof of Theorem 10 is then achieved as for [5, Theorems 6 and 7].